

Wearable Technologies Enable High-performance Textile Supercapacitors with Flexible, Breathable and Wearable Characteristics for Future Energy Storage

Jianfeng Wen¹, Bingang Xu^{1*}, Yuanyuan Gao¹, Meiqi Li¹, Hong Fu²

¹Nanotechnology Center, Institute of Textiles and Clothing, The Hong Kong Polytechnic University, Hong Kong, P.R. China

²Department of Mathematics and Information Technology, The Education University of Hong Kong, Hong Kong, P.R. China

*Corresponding author; Email: txubg@polyu.edu.hk

Abstract:

Flexible and wearable energy storage devices are expected to provide power support for the burgeoning smart and portable electronics. In particular, textile substrate and wearable technology derived supercapacitors (TWSCs) bear the inherent merits of high flexibility, stretchability, washability and compatibility over the non-textile devices, therefore, attract the excitement for achieving high performance and truly wearable energy storage products. In this review, the fundamental mechanisms of supercapacitor and typical technologies of wearable textiles are presented, with emphasis on the main advantages and progress of TWSCs. In view of the current challenges of TWSCS, we propose the strategies for the performance improvement, with expectation to open new avenues to promote the future development of the flexible and wearable supercapacitors.

Key words: wearable technology, supercapacitor; textiles; energy storage

Wearable Technologies Enable High-performance **Textile Supercapacitors** with Flexible, Stretchable and Wearable Characteristics for Future Energy Storage

Abstract:

Flexible and wearable energy storage devices are expected to provide power support for the burgeoning smart and portable electronics. In particular, textile substrate and wearable technology derived supercapacitors (TWSCs) bear the inherent merits of high flexibility, stretchability, washability and compatibility over the non-textile devices, therefore, attract the excitement for achieving high performance and truly wearable energy storage products. In this review, the fundamental mechanisms of supercapacitor and typical technologies of wearable textiles are presented, with emphasis on the main advantages and progress of TWSCs. In view of the current challenges of TWSCS, we propose the strategies for the performance improvement, with expectation to open new avenues to promote the future development of the flexible and wearable supercapacitors.

Key words: wearable technology, supercapacitor; textiles; energy storage

1 Introduction

The increasing booming of smart garments and portable electronics has put forward demands for flexible and wearable energy storage devices ^[1-4], such as the solar cells, metal-ion batteries, supercapacitors (SCs), etc ^[5-8]. These flexible energy storage systems are also promising to power the specific applications, like medical biomonitoring and military equipment ^[9-16]. As compared to batteries that are limited by the sluggish charging/discharging rate, SCs can show much higher power density and thus are popular with the researchers. In addition, textile industry is a worldwide traditional pillar industry that possesses a wide range of the maturity technologies. It

is, therefore, beneficial to develop the flexible SCs from the perspective of textiles and the manufacturing technologies ^[17-22].

Reviewing the reported works, focuses tend to be paid more on the plain concept of the flexibility, and less studies follow with interest on the achievements of TWSCs ^[23-25]. To date, a commercial TWSC does not exist, meaning still a lot of work needs to be done. In this review, we put emphasis on the superiority of TWSC and optimization strategy for the current defects, for the purpose of highlighting the significance of incorporating wearable textile technologies into SC development. Based on the thinking, this review begins with an introduction of the SC working principle and background information, followed by an overview of the typical textile substrate and manufacturing technologies. Thereafter, the merits of TWSCs are highlighted by reviewing the progress of the recent studies. To cope with the existing challenges of TWSCS, we then propose the strategies for improving the overall performance. This review provides an overview focusing on the textile substrate and wearable technologies derive SCs, aiming to apply the textile based research philosophy to guide the studies for the next-generation energy storage devices.

2 Principle and Background of Flexible SCs

2.1. Energy Storage Mechanisms

As shown in Fig.1, a flexible SC is typically composed of two flexible electrodes, solid/gel-state electrolyte, and the separator. When charged, SC stores the electrical energy via two typical ways, the electrostatic double layer capacitance and pseudocapacitance, corresponding to the electrical double layer capacitor (EDLC) and pseudocapacitor (PDC) ^[26, 27].

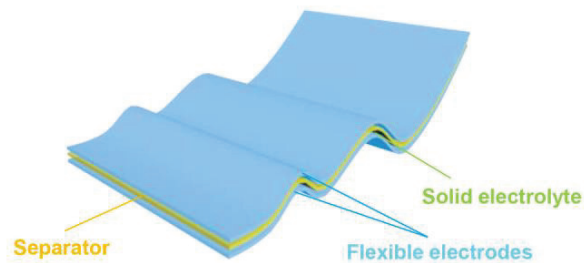


Fig.1 Schematic diagram of a flexible SC.

In principle, an EDLC stores charge relying on the electrostatic double layer formed by the reversible adsorption of electrolyte ions onto the charged electrode material [28-30], as shown in Fig.2.(a). For PDC, which was first presented by Conway in the 1970s, the electrical energy is not only stored by the electrostatic double layer, but also the fast surface redox reaction (or intercalation) [26, 31, 32], as shown in Fig.2.(b). Owing to the redox reactions, PDC shows higher charge storage while maintaining the comparable charging/discharging rates to the EDLC [23, 33-35]. The typical pseudocapacitive metal oxides include MnO_2 and RuO_2 , and they store charges via the surface insertion/deinsertion of the electrolyte cations and/or proton (H^+), and the general formula is show as below [30, 36]:



where M represents for metal elements, C^+ is the electrolyte cations (Li^+ , Na^+ , K^+ , etc.), a and b are the coefficients of cation and proton respectively.

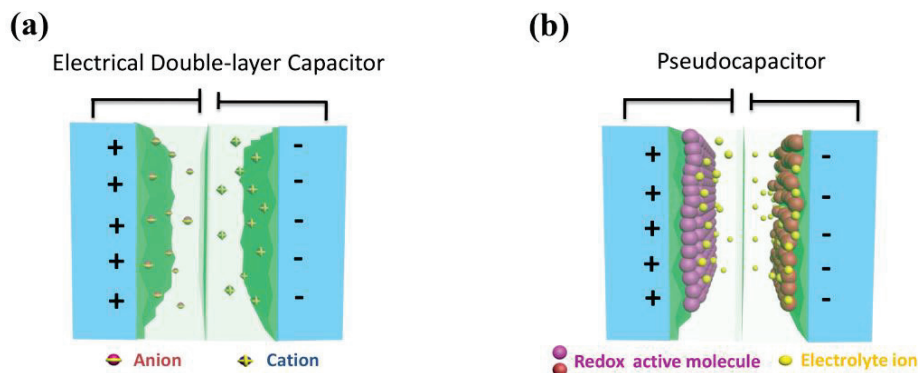


Fig.2 The schematic diagrams of (a) an EDLC and (b) a redox-type pseudocapacitor.

Based on the EDLC and PDC mechanisms, SC normally shows higher power density than that of the rechargeable batteries that store charges by the reversible redox reactions [37, 38]. Fig.3 shows the Ragone plot, which is presented for describing the relationship of power density versus energy density [39]. It is obvious that SC occupied the high specific power but low specific energy region, while batteries locate in the opposite area. The operation time constants well correspond to the energy storage devices, with tens of hours in the battery region and tens of seconds in SC area. The low power density of lithium-ion batteries (LIBs) is due to the reversible redox reactions occurred in the bulk of the electroactive material [40, 41]. The issues referring to anode Li-metal plating, the solid-state diffusion rate, and phase transformations severely restricted the charging rate and lifespan of LIBs [41, 42]. As shown in Fig.3, Patrice et al. defined the coloured solid areas as the performance derived at the same charging/discharging rate, while the dotted loops represented the performance calculated only by the discharge rate. By contrast, the wide blue region of SCs demonstrate higher power density than that of batteries, making SCs preferred for high power quality applications, like high voltage power correction and energy recovery in mass transit systems [30, 39, 43].

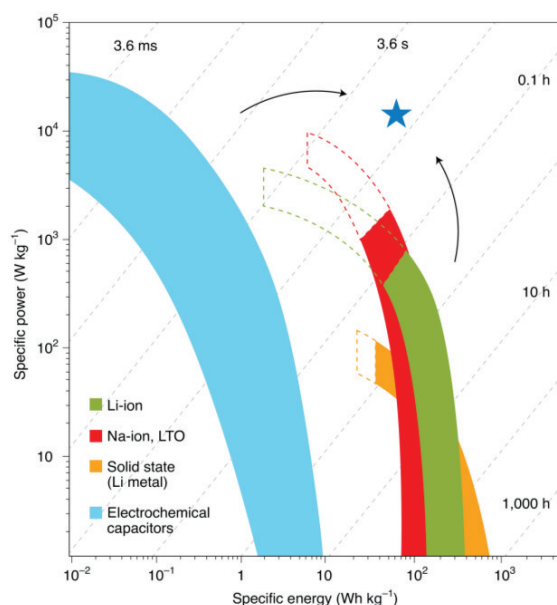


Fig.3 Ragone plot of different energy storage devices: specific power versus specific energy.
Reproduced with permission ^[39]. Copyright © The Author(s) 2020, Springer Nature Limited
2020

2.2. Metrics

The electrochemical measurements are normally performed at room temperature via an electrochemical workstation instrument in a three-electrode electrochemical cell, which consists of a piece of platinum plate and a reference electrode, and the as-prepared electrode. For the all-solid-state SC electrochemical measurement, one electrode of the SC acts as both the counter and reference electrode, while another electrode serves as the working electrode.

The cyclic voltammetry (CV), galvanostatic charge and discharge (GCD), and the electrochemical impedance spectroscopy (EIS) are applied to examine the electrochemical performance of the working electrode. The gravimetric capacitance derived from CV curves are calculated by the below equation ^[32, 44]:

$$C = \int i \, dV / (\nu m V) \quad (2)$$

where i , V , m , and ν , are the discharge current (A), the voltage window (V), the material mass (g), and the voltage scanning rate ($\text{mV} \cdot \text{s}^{-1}$). The energy density (E) and power density (P) of the device are calculated by the below equations ^[32, 45]:

$$E = CV^2 / (2 \cdot 3600) \quad (3)$$

$$P = 3600E / t \quad (4)$$

where C , V , and t , are the specific capacitance, the voltage window (V), and the discharging duration (s).

2.3. Flexible SCs

Along with the emergence of the portable electronics, such as rollup displays and bendable mobile phones, the flexible SC has been gaining momentum for power supply in a flexible manner ^[46]. The typical flexible SC configuration is shown in Fig.1, the flexible SCs display various advantages, such as the light weight, small size, high flexibility, good integration, etc. To date, substantial studies have reported on the research and development of the wearable SCs, in particular, the textile based substrates and wearable technologies, bearing the intrinsic flexibility and integration, received unique popularity in exploring the truly flexible SCs, as shown in Fig.4 ^[47, 48].

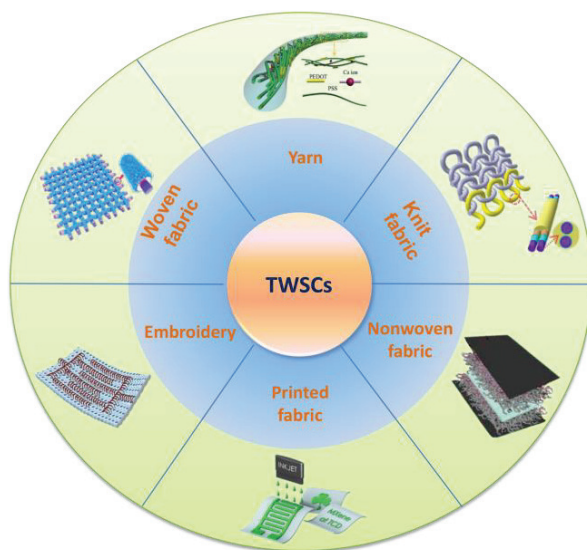


Fig.4 The schematic diagrams of TWSCs. Yarn SC image: Reproduced with permission ^[49]. Copyright 2015, Elsevier Ltd. Knit fabric: Reproduced with permission ^[50]. Copyright 2017 American Chemical Society. Embroidery image: Reproduced with permission ^[51]. Copyright 2019, Springer Nature Limited. Woven SC: Reproduced with permission ^[52]. The Royal Society of Chemistry. Nonwoven SC: Reproduced with permission ^[53]. Copyright 2015, Elsevier Ltd. Printed SC: Reproduced with permission ^[54]. Copyright 2019, Springer Nature Limited.

Yarn, produced by the spinning of natural and artificial fibers, presents the fundamental units of textiles and fabrics. By interlacing or interloping yarns, various

structures can be achieved by the fabrics. It is, therefore, rational and advantageous to initially develop the one dimensional (1D) fiber-shaped SCs (FSCs), followed by the production of the energy storage textiles with properties of small size, light weight, and great flexibility ^[17-22]. Consequently, the 1D SC devices can not only be developed to energy storage fabrics via various textile techniques (weaving, knitting, printing, etc.), but also be integrated into power systems with other devices. However, the main challenges of 1D SC lie in the use efficiency and layer protection of the electroactive material. By contrast, SCs assembled by the flat two-dimensional (2D) electrodes demonstrate higher working efficiency in using electroactive materials for storing energy ^[55]. Moreover, the textile-based fabric substrates, including the knit fabric, woven fabric, nonwoven fabric, and printed fabric, are among the ideal candidates for developing the truly flexible and wearable electrodes and SCs. Also, the 2D SCs can fit in easily with the common fabrics or garments, or even be fabricated directly as fabrics by utilizing textile manufacturing techniques. One disadvantage of the common fabric is the flat electrodes are normally incompatible with some 3D wearables. And thus, some special fabrics, such as the 3DSF, were accordingly selected for developing the 3D energy storage devices ^[56].

2.4. Electrode Materials

Normally, three types of the electroactive materials are widely adopted in the fabrication of the flexible SCs, including carbon-based materials, transition metal compounds and the conductive polymers ^[30, 57, 58]. Up to the very recent studies, plenty of novel materials were reported for the applications in wearable SCs, such as the polyoxometalates (POMs), metal-organic frameworks (MOF)-derived materials, etc ^[59]. Based on different synthetic principles, the electroactive materials are selectively fabricated in view of the specific textile technology. In the following context, the electrode materials are reviewed from aspects of the conventional and the novel electroactive materials.

2.4.1 Conventional Electroactive Materials

Carbon based materials. As the EDLC type, carbon-based SCs normally show very high power density and long cycling life, owing to the merits of high conductivity, light weight, low cost, large surface area, excellent thermal and chemical stability [60, 61]. Hence, the carbon based materials have been extensively used for constructing TWSCs, such as the activated carbon (AC), carbon nanotubes (CNTs), carbon fibers (CFs), graphene and its derivatives. As compared to pseudocapacitive materials, carbon-based materials cannot only serve as the electrode materials, but also be used as the flexible substrates and current collectors. Moreover, some of the carbon based materials were pretreated for enabling functional groups for gaining pseudocapacitance, such as graphene oxide (GO). The endowed functional groups on the carbon rings, such as the hydroxyl (C-OH) and carboxyl (COOH), can not only provide stronger stability for the 2D layered structure, but can also react with the electrolyte ions, storing electrochemical energy via the pseudocapacitive behaviors [62].

Transition metal compounds. Transition metal oxides are widely investigated in TWSCs for bearing the pseudocapacitive behaviors, and the typical oxides include RuO_2 , Fe_2O_3 , MnO_2 , NiO , Co_3O_4 , etc. [34, 63]. For example, the theoretical capacitance of RuO_2 is estimated to be nearly $2,200 \text{ F}\cdot\text{g}^{-1}$, and MnO_2 is around $1,370 \text{ F}\cdot\text{g}^{-1}$ [64, 65]. However, their poor electrical conductivity inevitably led to very limited mass loadings for fabricating the real SC devices, and eventually restricted the applications in the practical use. By using methods like hydrothermal method and electrodeposition, the transition metal oxides or hydroxides can be loaded on the flexible textile substrates. To improve the mass loadings of the electroactive materials, studies were largely devoted into fabricating versatile crystalline forms, designing porous structures, and synthesizing composite materials [66-68]. Moreover, the ternary transition metal oxides, such as NiCo_2O_4 , CoMoO_4 , $\text{Ni}_3\text{V}_2\text{O}_8$, etc., were also studied for gaining higher electrochemical performance [69-72]. Nevertheless, the electrical

conductivity still cannot break through the specific ranges of the transition metal oxides [73]. Consequently, the corresponding transition metal nitrides, carbides, sulfide, and phosphides were brought forward in terms of the high conductivity and low cost [74]. For example, vanadium nitride (VN) showed a high specific capacitance of 1,340 $\text{F}\cdot\text{g}^{-1}$ [75], when assembled with a ZnCo_2O_4 positive electrode, the asymmetric SC achieved a high specific capacitance of 196.43 $\text{mF}\cdot\text{cm}^{-2}$, and a volumetric energy density of 64.76 $\text{mWh}\cdot\text{cm}^{-3}$ [76]. Notably, 2D transition metal carbides or nitrides (denoted MXene) are emerging with promising prospect for energy storage, owing to the high electrical conductivity and fast reversible redox reactions with cations of Li^+ , Na^+ , K^+ , etc., and the pseudocapacitive behaviors of MXenes were reported to be over 900 $\text{F}\cdot\text{cm}^{-3}$ in aqueous electrolytes [77]. However, MXenes have flaws in operating voltage window, with only about 0.6 V, compared to the normal value of MnO_2 with 0.8 V.

Conductive polymers. Conductive polymers have either metallic conductivity or semiconductors' properties, as they are fabricated by incorporating polymer matrixes with nanofillers that are either conducting or insulating [78-80]. Due to the outstanding synergistic effects of the matrixes and nanofillers, conductive polymers are poised in a wide variety of areas, such as light-emitting diodes, artificial muscles, sensors and energy storage devices [81-83]. The most commonly used conductive polymers in PDCs include polyaniline (PANI), polypyrrole (PPy) and poly(3,4-ethylenedioxythiophene) (PEDOT), which have been largely explored in TWSCs via the electrochemical oxidation on the textiles. Particularly, their potential in doping levels within the tunable structures makes them a feasible candidate for fabricating composite electrode with other active materials [84]. In doing so, the redox reactions that occurred around the electrode surface area can conduct deeply even in the bulk of the electrode, contributing greatly to the capacitance and energy density. However, the accompanying negative effects can decrease the power density and cycling life [85].

2.4.2 Novel Electroactive materials

Polyoxometalates (POMs). A new class of 3D structured molecular clusters with oxygen and transition metals (W, Mo, V, etc.) at the highest oxidation states are emerging as the novel electroactive material for energy storage [86]. These nanometric POMs, with the general formula $H_nAM_{12}O_{40}$ (A: Si/P, M: W/Mo/V), showed ample reversible redoxes and were well fit to gain high electrochemical performance energy storage devices. Typically, POMs are categorized as Keggin type, phosphomolybdate (PMo_{12}) and phosphotungstate (PW_{12}), which present the MO_6 (M: W/Mo) moieties on the surface, making them the ideal pseudocapacitive materials for constructing SCs [87].

MOF-derived material. Owing to the substantial porosity and the adjustable pore size, MOFs were considered with significant potential in fabricating electrode of SCs. Specifically, MOFs are usually fabricated on the flexible and conductive substrate (eg.: carbon fibers), followed by a general carbonization process for gaining the porous structure with high electrical conductivity. For instance, MOF-5-derived carbons were fabricated and assembled for a SC, displaying an energy density of $17.37 \text{ Wh} \cdot \text{kg}^{-1}$ at the power density of $13 \text{ kW} \cdot \text{kg}^{-1}$, and the capacitance retention was nearly 94.8% after 10,000 cycles in $\text{Na}_2\text{SO}_4/\text{PVA}$ gel electrolyte [88]. To further apply MOFs in SCs, some other materials with high conductivity, such as CNTs, rGO, PPy, PANI, etc., were also interwoven with MOFs for gaining synergistic properties [89, 90].

Black phosphorous (BP). As the prosperous development of 2D materials, BP was presented as one of the most stable allotrope of phosphorous. Similar to the common 2D materials, BP is made up of the puckered-layer structure of P atom planes via van der Waals interactions, which can be obtained by both mechanical and liquid exfoliation [91]. Furthermore, BP displays a similar layer spacing distance of 5.3 \AA , higher than that of the graphite with 3.6 \AA , showing great values and potential in the application for energy storage [92]. Recently, Wen et al. fabricated the novel BP

sponges via the electrochemical exfoliation of the bulk BP crystals. By using the tetrabutylphosphonium bromide electrolyte, the oxidation side reaction of BP was well prevented, and the resulting SC showed a gravimetric capacitance of $80 \text{ F} \cdot \text{g}^{-1}$ at $10 \text{ mV} \cdot \text{s}^{-1}$, larger than the original bulk BP crystals ^[93].

Others. Apart from the above-mentioned electroactive materials, some other specific compounds were applied in TWSCs, owing to either high specific surface area, or excellent electrochemical performance. For instance, bismuth chalcogenide manifested the fast reversible redox behavior, and the composites of Bi_2S_3 and graphene were prepared by Nie et al., achieving a gravimetric capacitance of around $396 \text{ F} \cdot \text{g}^{-1}$ at $1 \text{ A} \cdot \text{g}^{-1}$ in the 2 M KOH aqueous electrolyte ^[94]. Also, Pan et al. adopted a strategy of purposely fabricating co-doping $\text{Mn}_x\text{Mo}_{1-x}\text{S}_{2-y}\text{Se}_y$ and $\text{MoFe}_2\text{S}_{4-z}\text{Se}_z$ nanosheets on the flexible carbon cloth as the positive and negative electrode respectively. And the resulting asymmetric SC demonstrated an energy density of nearly $69 \text{ Wh} \cdot \text{kg}^{-1}$ at the power density of $0.985 \text{ kW} \cdot \text{kg}^{-1}$ ^[95]. As compared to S/Se based transition metal compounds, the corresponding tellurides demonstrated much higher electrical conductivities, showing a promising future in the development of SCs.

3 Fundamental Textiles and Technologies

3.1 Yarns

Yarns are composed of the interlocked fibers, such as the staple and filament fibers. By performing different textile technologies, yarns serve to produce knitwear, embroidery, woven and nonwoven fabrics, etc. ^[2]. Generally, yarns are usually made into spun yarns, filament yarns, and their composite before using. According to the twisting degrees, yarns are also divided into single-ply yarn and multi-ply yarn ^[96], as shown in Fig.5.

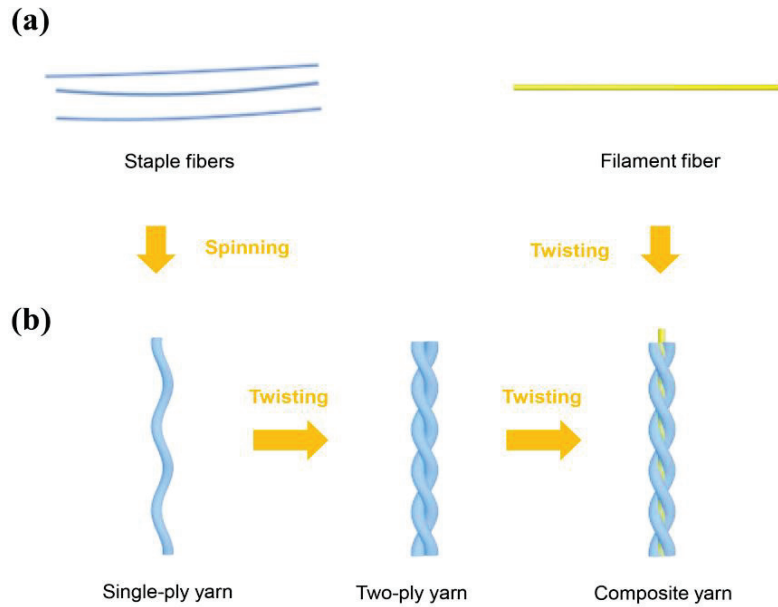


Fig.5 The schematic diagram of a flexible SC

Apart from the conventional yarns, various functional yarns have been introduced to the market to assist the rapid development of the smart textiles, such as the metallic yarns (eg.: stainless steel yarn, aluminum yarn), metal-plated yarns (eg.: silver-plated yarn), and the carbon-based materials yarns (carbon fibers) ^[97]. In the presence of these new yarns, textiles can not only show the conventional physical properties, but also the decent electrical conductivity and mechanical strength. In this regards, different yarns are usually adopted for producing fabrics with various functions, such as the silver-plated yarns knit conductive fabric ^[98], the carbon fiber based high-strength nonwoven felt ^[99].

3.2 Fabrics

3.2.1 Knit Fabric

Knitting is an ancient and classic textile technology that intermeshes loops of either a single yarn or groups of yarns together. When a single thread is used for loops taking place in a width direction, the process is named weft knitting. Similarly, when the threads are laid in a length direction, the corresponding process is known as the warp

knitting, as shown in Fig.6.(a) and (b).

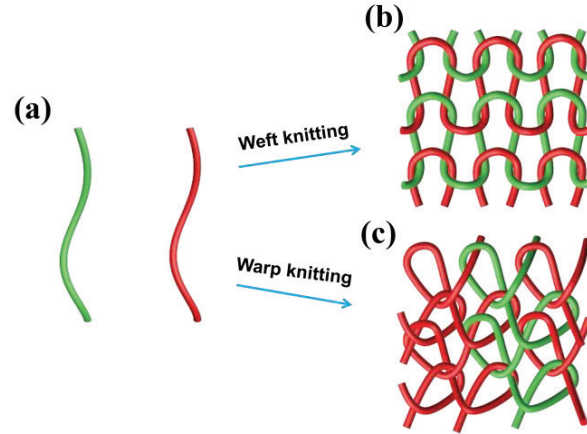


Fig.6 The schematic diagrams of (a) weft knitting and (b) warp knitting.

In the conventional hand knitting, loops are obtained by pulling through a yarn from a row of stitches to another. As in the machine knitting, each needle is responsible for its own stitch, pulling the yarn through the old loop to form the new stitch. Thus, the characteristics of knit fabrics are normally affected by the applied yarns and techniques, such as the yarn color, stitches, interlace and the machine gauge ^[100].

3.2.2 Woven Fabric

Similar to the knit fabric, a woven fabric is likewise composed of the warp and weft threads, as shown in Fig.7. Specifically, a woven fabric normally involves three main steps. Firstly, the warp threads are raised in two layers to create an open area (called the shed). Secondly, the filling yarns are inserted through the shed via the shuttleless, known as picking. Afterwards, the process is named beating, which aims to push the filling yarns into the already woven fabric by the reed ^[101]. To control the weaving process precisely, it is essential to regulate the yarn delivering motion at the suitable rate and the constant tension. The loom is adopted for keeping the warp threads evenly spaced and under tension.

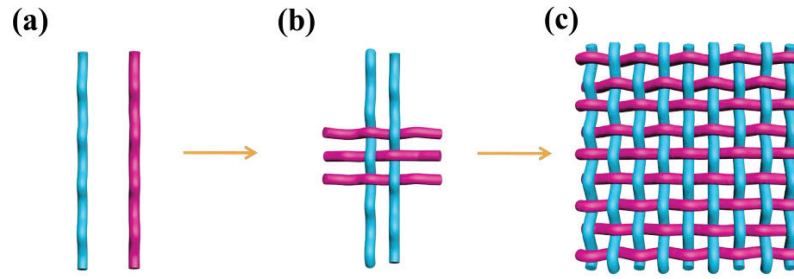


Fig.7 The schematic diagram of the woven fabric.

Nowadays, as the development of textile industry, various complex structures constructed woven fabrics are readily achieved by using the modern weaving machines, and thus, distinctive characteristics, such as appearance, feel, and performance, are endowed to the composite fabrics ^[102].

3.3.3 Nonwoven Fabric

Originally, the nonwoven fabric emerged against the woven fabric, up to today, the nonwoven technology has become one of the most widely used methods in textile industry ^[103]. Unlike the woven and knit fabrics, which are formed gradually via the programmatic process, the nonwoven fabrics are usually achieved via the direct compressing manufacturing, with both random and oriented fiber arrangements, as shown in Fig.8.(a), (b) and (c). Thus, the non-woven fabrics normally have a compact structure can be tailored without fraying, and this is a unique merit than cannot be provided by both knit and woven fabrics

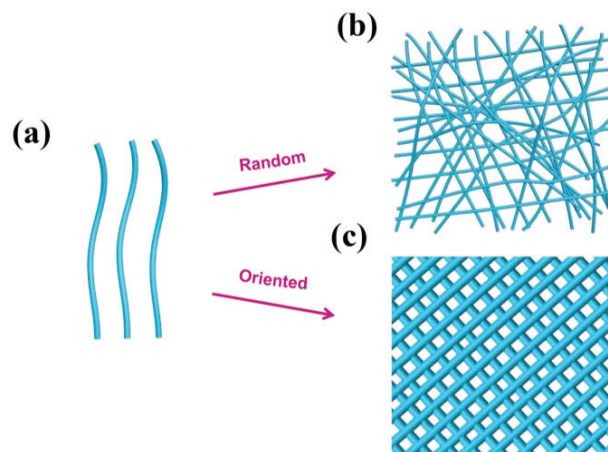


Fig.8 The nonwoven fabric diagrams of (a) the random arrangement, (b) the oriented arrangement

Instead of using the conventional textile processing, such as carding, roving, spinning, etc., the nonwoven processing exclusively involves steps of web formation and bonding, finishing and converting, etc. ^[103]. Recent years, to meet the demand of the new market, various new materials that possess unique chemical and physical properties are adopted to enable the nonwoven fabrics with multi-functions ^[104].

3.3.4 Printed Fabrics

The main coating or printing techniques in textile industry are dyeing and screen printing. Unlike the conventional dyeing that makes the whole fabric covered with colors, fabric printing focuses only on the certain parts for a sharply defined design. Fig.9 shows the schematic diagram of the printed fabric. In the typical printed fabrics, colors are well bonded with the internal textile fibers, which makes it greatly favorable to resist washing and friction ^[105]. In terms of coloring the specific areas of a fabric, rich and varied dyes, pigments and paints are applied in combinations for gaining the desired fabric appearances. Normally, the printed appearance is affected by several elements: the base fabric types, the design and the fabrication, and the dyestuffs types.

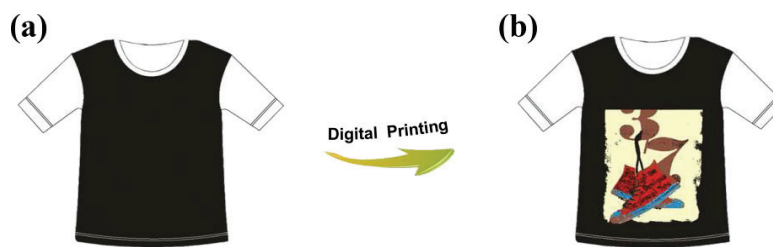


Fig.9 The diagram of the digital printing

According to the printing mechanism, four ways are mainly exerted for gaining the fabric, including dyeing, resist, discharge and direct. Specifically, dyeing is realized by immersing the fabric into a bath of dye solution, with a colored pattern finally

printed on the fabric ^[106]. Resist is close to a template method that prevents some areas of the fabric from being taken up by the dyes, retaining the original appearance. Color discharge is a way to substitute the original color with a new one in the same printing process. Direct printing means to coat the colorant merely on the fiber surfaces rather than the internal fibers ^[107]. Hence, the desired patterns are able to be properly achieved via an appropriate selection on the printing method.

3.3.5 Sewn Fabrics

Sewing is one of the oldest techniques carried out by passing through yarns or threads into the fabrics for joining or repairing cloth pieces. As the development of the first Industrial Revolution, sewing machine was invented to improve the working efficiency and reduce the manual sewing work in clothing companies ^[108]. As compared to the unmanned automatic operation, like knitting and weaving, sewing is more applied to construct or decorate fabrics for specific purposes. Sewing machine can normally realize both basic and specific stitches. For instance, basic stitches include straight stitches, zigzag stitches, stretch stitches, and blind stitch or other hemming stitches ^[109]. For a specific requirement, sewing machine can perform the decorative stitching to create versatile patterns on the base fabric, as shown in Fig.10. Although the sewing machine has dominated the manufacturing field, a number of the specific fabrics cannot be sewn by machines, thus, the traditional hand sewing is still preserved for providing some special use, in particular, hand sewing can also bring precise and decorative stitches, which is more advantageous for processing smaller products ^[110].

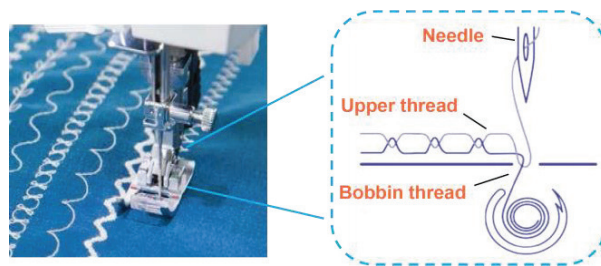


Fig.10 The schematic diagram of the sewing machine.

3.3.6 Embroidery

Handmade embroidery, evolved from the conventional hand sewing with a long history of thousands of years, is widely adopted for the purpose of gaining ingenious and fancy creations in art or design. Owing to the solid foundation of the modern information technology and the mechanical automation, the computer-aided embroidering has made substantial progress, showing much higher precision and productivity than that of the hand embroidering, as shown in Fig.11 ^[111]. Compared to the conventional sewing technique, what differs is that the modern embroidering favors to construct more ornate and complicated patterns by using the computerized programming, which is capable of both designing the patterns and precisely control of the whole production. In addition, beyond the basic weaving and knitting techniques, embroidering also shows merits in the perspectives of integration, customized design, etc., like the patch embroidered antennas and vias ^[112]. Therefore, the advances of the embroidering technique will be highly beneficial for the development of the future electronic textiles (E-textiles).

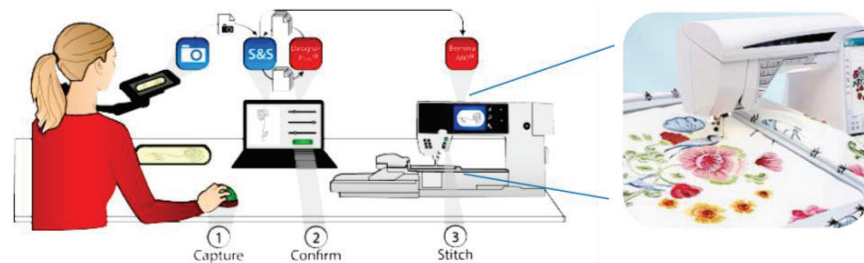


Fig.11 Diagram of the computer-aided embroidering. Reproduced with permission. Copyright

© The Author(s) 2019 ^[111]

3.3.7 3D Spacer Fabrics

Three dimensional spacer fabric (3DSF) is one special type mainly used in the composite industry ^[113]. Generally, 3DSFs serve as the reinforcement materials combined with several matrices to obtain the textile structural composites. Compared to the commonly used engineering materials, such as metals and ceramics, the textile structural composites usually possess higher mechanical properties and lower density,

and thus, they are widely employed in civil engineering and military industry ^[114]. Moreover, taking the delamination resistance and damage into account, the 3DSF derived textile composites can exhibit more advantages than the conventional unidirectional composites ^[115].

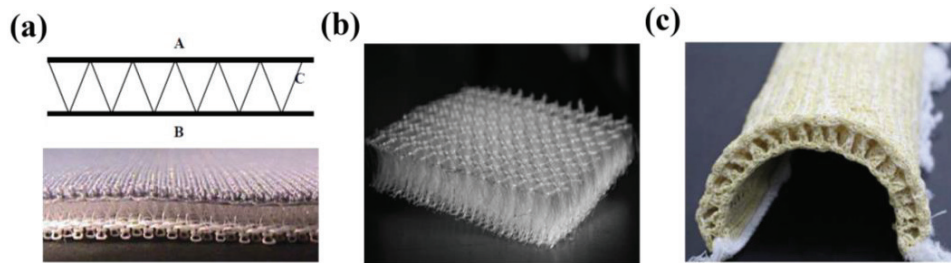


Fig.12 The real photos of (a) weft knit spacer fabric ^[116], (b) polyester-made 3DSF, (c) aramid fibers made 3DSF with 180°curvature ^[117].

Based on different textile techniques, 3DSF can be achieved in many ways, such as weaving, knitting, stitching, and even nonwoven techniques. As shown in Fig.12.(a), the basic 3DSF is realized via the one-pot construction, where the two separated fabric layers (A and B) are connected with the fibers of the spacer layer (C). Thanks to the unique three-layer sandwiched structure, the 3DSF usually shows superiority in stable structure, high breathability, great compression withstanding, etc. ^[118]. Fig.12.(b) shows the typical polyester 3DSF with a higher thickness than the common fabric, and it is mainly applied in cushioning or impact protection ^[48, 119]. Notably, by using soft fibers and yarns (cotton, nylon, etc.), the resulting 3DSF demonstrates great flexibility. As shown in Fig.12.(c), the aramid fibers made 3DSF can be bended to nearly 180° curvature ^[117]. Recent years, as the advances of the E-textiles, 3DSF has been applied in the interdisciplinary applications, such as the piezoelectric and triboelectric nanogenerators ^[98, 120], and it is believed that there is a tremendous potential to develop more 3DSF based smart devices.

4 Main Advantages and Progress of TWSCs

For the development of wearable supercapacitors, plenty of the flexible substrates

were explored and studied, for example, the carbon materials (carbon fibers) and metallic foils (Cu foil and Ti foil) displayed impressive conductivity and stability, and the polymer films (PET) showed excellent mechanical strength ^[121, 122]. Nonetheless, SCs made by these substrates often suffer from the limited wearability, such as the poor flexibility and weak compatibility, which are almost the fatal flaws of a wearable energy storage device. By contrast, TWSCs naturally inherit the intrinsic advantages of textiles, bearing true flexibility, excellent breathability, natural compatibility and even similar processing. Therefore, it is of great significance to develop flexible SCs from the perspective of textile substrates and the related technologies. With a focus on the advantages of TWSCs, this section reviews the recent progress of TWSCs studies, and discusses the major challenges and solutions to TWSCs accordingly.

4.1 Flexibility

As compared to the widely used metallic foil substrate, TWSCs have the intrinsic ultrahigh and true flexibility, owing to the natural softness of the textile fibers and the fabric interlacing structures. One dimensional (1D) fiber-shaped SCs with a high aspect ratio usually have great flexibility, and their 1D tractable structure can also facilitate the subsequent integration with the end products. As for the two dimensional (2D) fabric SCs, the fabric features of low fiber density and small thickness are contribute to the advancement of the device flexibility greatly. Nevertheless, the 3D fabrics only showed limited flexibility in the horizontal direction, due to their high thickness.

4.1.1 Fiber-shaped SCs

The design of fiber-shaped electrode mainly includes two major strategies: core-sheath structured design and the material integration configuration, as shown in Fig.13.(a) and (b). For the fabrication of the core-sheath 1D electrode, the soft textile fibers are normally as the supporting core, while the electroactive materials serve as the sheath. For an integrated electrode, it is mainly realized by using only one

precursor solution containing both conductive and electroactive materials. However, both of the two electrodes showed impressive advantages in flexibility and mechanical strength.

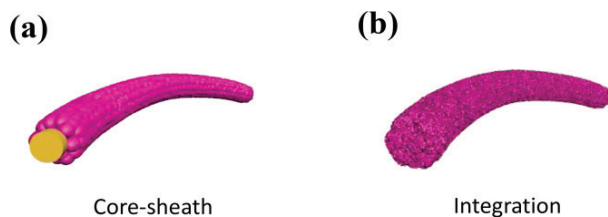


Fig.13 The typical fiber-shaped electrode: (a) core-sheath structure, (b) materials integration structure

In terms of different electrode fabrications, fiber-shaped SCs normally have three assembling forms, including the parallel, twisted, and coaxial structures, as shown in Fig.14.(a), (b), and (c).

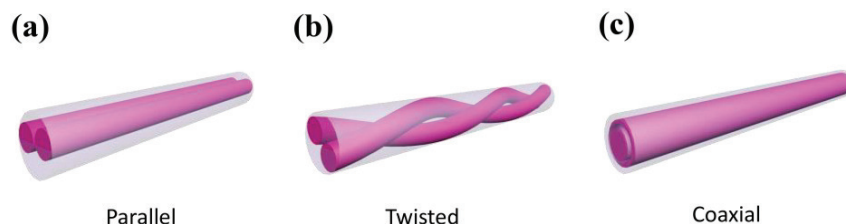


Fig.14 The assembling forms of fiber-shaped TWSC: (a) parallel, (b) twisted, (c) coaxial

In the core-sheath fiber-shaped electrode, the highly conductive fibers or yarns were preferably selected as the core for providing efficient current, such as the carbon based fibers, metallic fibers, and the metal-plated yarns. Owing to small and uniform fiber fineness, most of the conductive core displayed great flexibility ^[123]. To construct the device, carbon based fibers are readily assembled as the EDLC-typed SC, while the electroactive materials are mainly fabricated as the sheath. By performing the core-sheath strategy, very low interface resistance is normally achieved, which is advantageous for the electron transferring into the electroactive materials, maximizing the overall electrochemical performance. Our previous studies

adopted the electrodeposition successfully grew the nickel/cobalt oxides and nickel/cobalt sulphides on the stainless steel yarns (SSY) as the positive electrodes, respectively, showing very high specific capacitances and voltage windows. In addition, both of the two device displayed great flexibility, the PPy@SSY//NiCoO₂@SSY SC retained its capacitance above 99.8% after bending the device at various degrees, and the rGO@SSY//NiCo₂S₄@SSY SCs were hand-sewn on a fabric with the flower pattern in series and successfully powered a LED, indicating excellent flexibility and application prospect ^[47, 124].

To facilitate the insertion of the fiber-shaped SC to the end product, the twisted and coaxial assembling forms are more popular with the development of 1D flexible energy storage device. Based on the core-sheath electrode, Shen guozhen's group developed a carbon fibers (CFs) @ CoNiO₂ positive electrode, as shown in Fig.15.(a). By pairing an activated carbon@CFs negative electrode in a twisted assembly, the 1D SC showed a gravimetric capacitance of 795.4 F·g⁻¹ at the current density of 2 A·g⁻¹. The twisted SCs were then covered by polydimethylsiloxane (PDMS), and successfully integrated into the real garment. By fabricating a 1.2 m long device, the 1D SCs were readily woven as the straw hat, watchband and the waistband ^[125]. As compared to the twisted SC, the coaxial SC structure has merits in large electrode contact area and small device width, which are more beneficial for the device integration. As shown in Fig.15.(b), the CNT fibers were grown VN nanowires arrays (NWAs) as the inner electrode, followed by a layer of the polyvinyl alcohol (PVA) electrolyte. CNT sheets were then encapsulated onto the electrolyte for as the outer tubular electrode. With the PEDOT:PSS and MnO₂ as the electroactive materials, the coaxial SC showed a high voltage window of 1.8 V, as shown in Fig.15.(b)-i. In addition, the coaxial structure demonstrated excellent flexibility (Fig.15.(b)-ii), and the SC was easily tied into a knot as the same as a normal natural fiber. By performing the bending test from 0 ° to 180 ° for 5,000 cycles, the device showed a high capacitance retention of 96%, and the device was successfully sewn onto a toy (Fig.15.(b)-ii), displaying the comparable stitchability to the normal yarns ^[126].

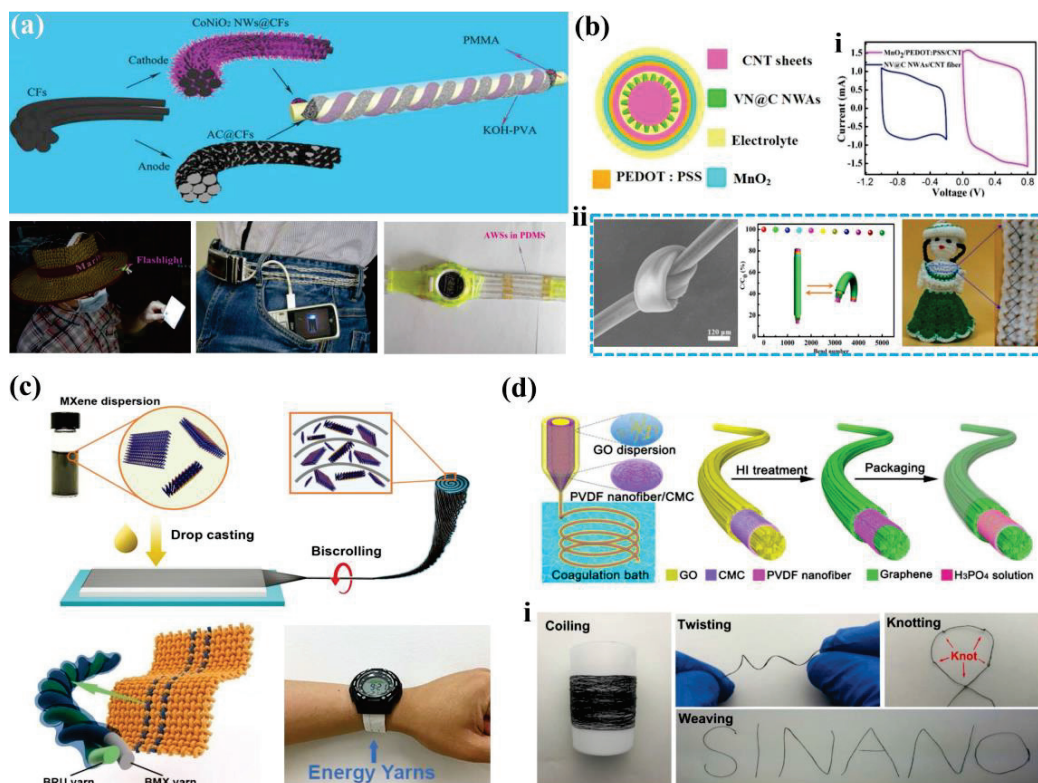


Fig.15 (a) The diagram of the $\text{CoNiO}_2\text{@CF//AC@CF}$ twisted device. Reproduced with permission ^[125]. Copyright © The Author(s) 2016, Wiley VCH. (b) The sketch of 1D coaxial SC: i: CV curves of positive and negative electrodes, ii: test and demonstration of the SC flexibility. Reproduced with permission ^[126]. Copyright © The Author(s) 2017, American Chemical Society. (c) The diagram of the $\text{MXene@CNTs//RuO}_2\text{@CNTs}$ integrated SC. Reproduced with permission ^[127]. Copyright © The Author(s) 2018, Wiley VCH. (d) The integrated coaxial $\text{graphene@PVDF nanofiber@graphene}$ SC: i: real photos of the fiber deformations. Reproduced with permission ^[128]. Copyright © The Author(s) 2020, Elsevier Ltd.

Apart from the core-sheath strategy, the integrated electrode is usually fabricated directly by the conductive and electroactive materials, and it is therefore capable of loading higher mass of the electroactive materials ^[129]. As an one-pot fabrication strategy, the electrospinning and wet spinning methods have been widely used in the integrated electrode ^[129-132]. For example, Yury's group reported an electrospinning of the bistrapped MXene and CNTs sheets, as shown in Fig.15.(c), CNTs were well

intermingled with MXene nanoplates, and the electrospun electrode can be well knotted as the same to the natural fibers. By pairing a $\text{RuO}_2@\text{CNTs}$ positive electrode, a twisted asymmetric SC was finally achieved, expressing a high energy density of $168 \mu\text{Wh}\cdot\text{cm}^{-2}$ at the power density of $14.8 \mu\text{W}\cdot\text{cm}^{-2}$. Two pairs of the SCs were then woven into a 100-thread count cotton fabric, and successfully powered the digital watch. The bending test showed that the capacitance was kept well after 1,000 cycles [127]. Similarly, the coaxial strategy is also applicable to the integrated electrode. Li et al. adopted the wet spinning method fabricated a coaxial SC, with the poly(vinylidene fluoride) (PVDF) nanofiber separator tightly sandwiched by the graphene fibers, as shown in Fig.15.(d). The obtained architecture with the interconnected and wrinkled network provided the coaxial graphene@PVDF nanofiber@graphene SC with an areal capacitance of $346.5 \text{ mF}\cdot\text{cm}^{-2}$ and energy density of $30.8 \mu\text{Wh}\cdot\text{cm}^{-2}$. As displayed in the real photos of Fig.15.(d)-i, the fiber-shaped coaxial SC demonstrated very high endurance to the deformations of coiling, twisting, and knotting, implying impressive flexibility and weaveability [128].

4.1.2 Fabric SCs

Different from the fiber-shaped SCs, whose flexibility is sometimes subjected to the end product integration, the two dimensional (2D) fabric SCs are usually achieved by the direct decoration of the fabric, and thus, their exceptional features can contribute greatly to the advancement of the 2D SC flexibility. Specifically, the knit fabrics feature characteristics of low fiber density and large pores, while the woven fabrics are regularly processed with the the warp and weft threads. Both of them have been substantially reported for fabricating flexible SCs. In comparison, the nonwoven fabric manufacturing usually draw support from an adhesive or thermal binder, endowing the fabric with characteristics of high fiber density and gasproofness, and this can disproportionally degrade the flexibility and air permeability.

Knit fabric SCs. Knitting process mainly involves the intermeshing loops of yarns, with large numbers of pores and spaces well retained. This enables the fabric with

excellent air permeability and true flexibility ^[133]. Therefore, it is reasonable to use a knit fabric as the substrate of a flexible SC. Our previous work applied a two-step method fabricated the conductive knit cotton fabric, and the resulted SC showed a high energy density of $65 \mu\text{Wh}\cdot\text{cm}^{-2}$ at a power density of $0.4 \text{ mW}\cdot\text{cm}^{-2}$. The device demonstrated very stable power supply when measured at a wide range of the flexibility ^[134]. As for the truly flexible SCs, Yury and Genevieve, for the first time, reported the textile supercapacitors by screen printing the activated carbon paint onto the carbon fiber fabrics, as shown in Fig.16.(a). The knit and woven fabric were all

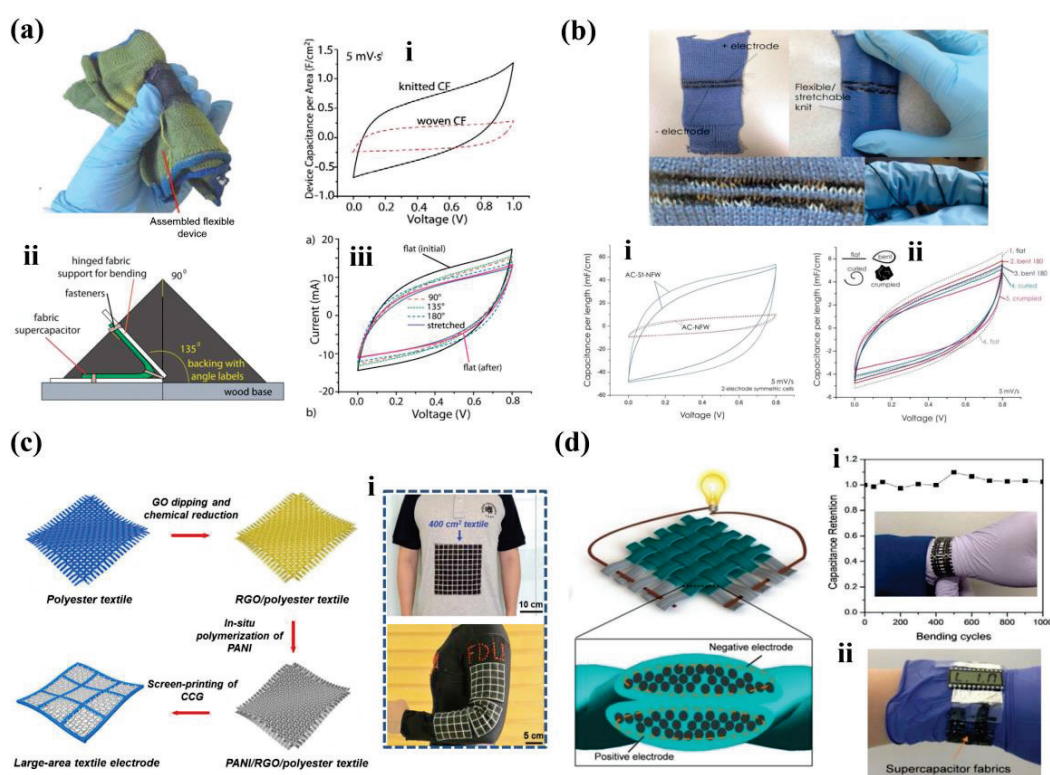


Fig.16 (a) Carbon fibers knit and woven SC: i: CV curves of knit CF and woven CF, ii: the diagram of the bending angles, iii: CV curves at different deformations. Reproduced with permission ^[135]. Copyright © The Author(s) 2013, The Royal Society of Chemistry. (b) MWCNT/MoO₃ coated knit fabric SC: i: CV curves of AC-St-NFW and AC-NFW, ii: CV curves at different bending degrees. Reproduced with permission ^[97]. Copyright © The Author(s) 2019, American Chemical Society. (c) Sketch of the woven fabric based PANI/RGO SC: i: the real photos of the energy storage T-shirt. Reproduced with permission ^[136]. Copyright © The Author(s) 2016, Wiley VCH. (d) The activated carbon fiber threads

woven SCs: i: the capacitance retention at different bending cycles, ii: the demonstration of SC powering a liquid crystal. Reproduced with permission ^[137]. Copyright © The Author(s) 2017, Springer Nature Limited.

tested as the flexible current collector, and the comparison of CV curves in Fig.16.(a)-i demonstrated that the knit device had better areal capacitance than the woven devices, which was attributed to different mass loading of the electroactive material. The examination of the flexibility was conducted following the principle in Fig.16.(a)-ii, and indicated very less changes of CV curves when bended from 90° to 180° (Fig.16.(a)-iii), meaning an impressive property in flexibility ^[135]. Subsequently, Yury's group continued the focus on the development of the functional yarns, and they fabricated a two-ply composite yarn by twisting the activated carbon (AC)-coated yarn with a stainless steel yarn (denoted AC-St-NFW). As shown in Fig.16.(b), the functional AC-St-NFW yarns, together with the non-conductive yarns (acting as a physical separator), were successfully knitted as the fabric device. For a comparison, the cyclic voltammograms of AC-NFW and AC-St-NFW yarns were performed and shown in Fig.16.(b)-i. It indicated that the gravimetric capacitance of AC-St-NFW yarn was high to 120 F·g⁻¹ (at 2 mV·s⁻¹), much better than that of the pure AC-NFW yarn (36 F·g⁻¹). The resulting knit fabric device was then tested in different bending states for understanding the flexibility, and it can be seen from Fig.16.(b)-ii, CV curves showed only limited capacitive decay upon the regular bending states, and the device can remain the original capacitance well when recovered to the flat state. The knit fabric and technique demonstrate a promising prospect for developing the truly flexible energy storage devices ^[97].

Woven Fabric SCs. Based on the warp and weft weaving mechanism, the woven fabrics usually bear higher fiber density than the knit fabrics, which normally renders more compact and sturdy features, but discounted flexibility. However, by applying much softer and more resilient yarns, woven fabrics can also display the convincing flexibility. For instance, Peng's group prepared a woven fabric SC by decorating a

polyester textile with rGO/silver paste and polyaniline (PANI) in order. As shown in Fig.16.(c), the textile based SC was readily scaled up to a size of 100 cm², demonstrating the capacitance, power, and energy of 69.3 F, 80.7 mW, and 5.4 mWh, respectively. Owing to the intrinsic flexible characteristic, the woven fabric SC was tested to be maintaining about 95.6% of the initial capacitance after bending at 90° for 1000 cycles. As shown the real photos in Fig.16.(c)-i, a large fabric SC of 400 cm² was successfully woven into a T-shirt, showing an ultrahigh stability at various deformations. Moreover, three SCs were then woven in series into a T-shirt, and finally lit up an “FDU” logo consisting of 44 LED ^[137]. In addition to use the woven fabric substrate, it is more challenging to directly weave a SC via the 1D electrodes. As an example in Fig.16.(d), the carbon fiber thread was firstly activated by KOH under N₂ annealing to gain a high porosity and hydrophilicity. Subsequently, the activated carbon fiber threads were woven as a fabric SC directly, showing a great flexibility. As indicated in Fig.16.(d)-i, the device retained the capacitance well after 1000 cycles of bending test, and it was then used as a watchstrap, and successfully powered a liquid crystal, as shown in Fig.16.(d)-ii ^[137].

Other fabrics and techniques were also reported for developing the flexible SCs, however, it could emerge some issues under different circumstances. An nonwoven fabric manufactured with the melting polymer binder may inevitably produce some rigidity ^[138]; an electrospun fabric originated from the polymer precursor can produce brittle fracture ^[139]; the printed device and embroidery normally show the flexibility subjected to the substrate; the 3DSF shows only inferior flexibility due to the higher thickness of the three-layer structure ^[116].

4.2 Stretchability

As a truly wearable device, only flexible and foldable properties are not enough to meet the practical demand. In particular, the stretchability is highly desirable for buffering the ubiquitous deformations generated by human daily activities. An

effective stretchable SC is capable of maximally sustaining its electrochemical performance when subjected to various strains. Based on the progress of the TWSCs, the 1D fiber-shaped SCs showed great advantages in high stretchability. By utilizing the intrinsically elastic fibers as the SC substrate, the 1D device can readily response to a certain degree of strain. Also, to prepare the fiber-shape electrode in a helical structure, the considerable stretchability can be achieved, even for the inelastic yarns. Moreover, according to the characteristics of different textile technologies, the knit fabric SCs with the intermeshing yarn loops usually demonstrated higher stretchability than those of the others, such as the printing and spraying strategies.

4.2.1 Intrinsically Elastic Fiber SCs

Stretchable fiber-shaped SCs can be directly achieved through the strategy of using the intrinsically elastic fibers, followed by the loading of the electroactive materials and the gel electrolyte in a proper way, the whole device can display varying degree of the stretchability. Wang's group successfully developed a stretchable coaxial-fiber SC by using the elastic polymer fiber substrate. They firstly wrapped the aligned CNT sheets onto the prestrained polymer fiber via the motor-based equipment, as shown in Fig.17.(a). After the combination with PEDOT:PSS and MnO₂ electroactive materials in order, a layer of the PVA gel electrolyte was attached onto the as-prepared electrode, resulting in the core electrode of the device. By wrapping another CNT sheets and electrolyte successively, a stretchable fiber-shaped coaxial SC was finally obtained. Benefiting from the skillful design of the coaxial structure, the SC delivered a high energy density of 1.42 mWh·cm⁻³, with the capacitance retention of nearly 85 % when stretched for 6000 times. As shown in Fig.17.(a) i and ii, the fiber-shaped device underwent a stretching test from the strain of 0 % to 200 %, and there were no severe changes occurred in the charging/discharging curves, indicating great flexibility and stretchability ^[140]. Similarly, an elastic urethane fiber served as the core fiber of the cotton spun yarn for enabling the stretchability. As shown in Fig.17.(b), by coating the CNT and polypyrrole (PPy) as the current collector and electroactive material

respectively, the symmetrically assembled device demonstrated high specific capacitance and rate capability. In particular, the relationship of SC electrochemical performance with the applied strain was studied in details. From Fig.17.(b) i and ii, it can be seen that the capacitances maintained above 85 % after a stretching test at a strain of 40 % for 1,000 times. As the strain increased to 80 %, the capacitance retention can still keep around 80 %. However, when the strain exceeded 100 %, there occurred severe IR drops in the discharging curves, which might be the reason of the damaged electrolyte. Nevertheless, this works still provided a novel and successful example for generating the stretchable fiber-shaped energy storage devices by using the textile materials ^[141].

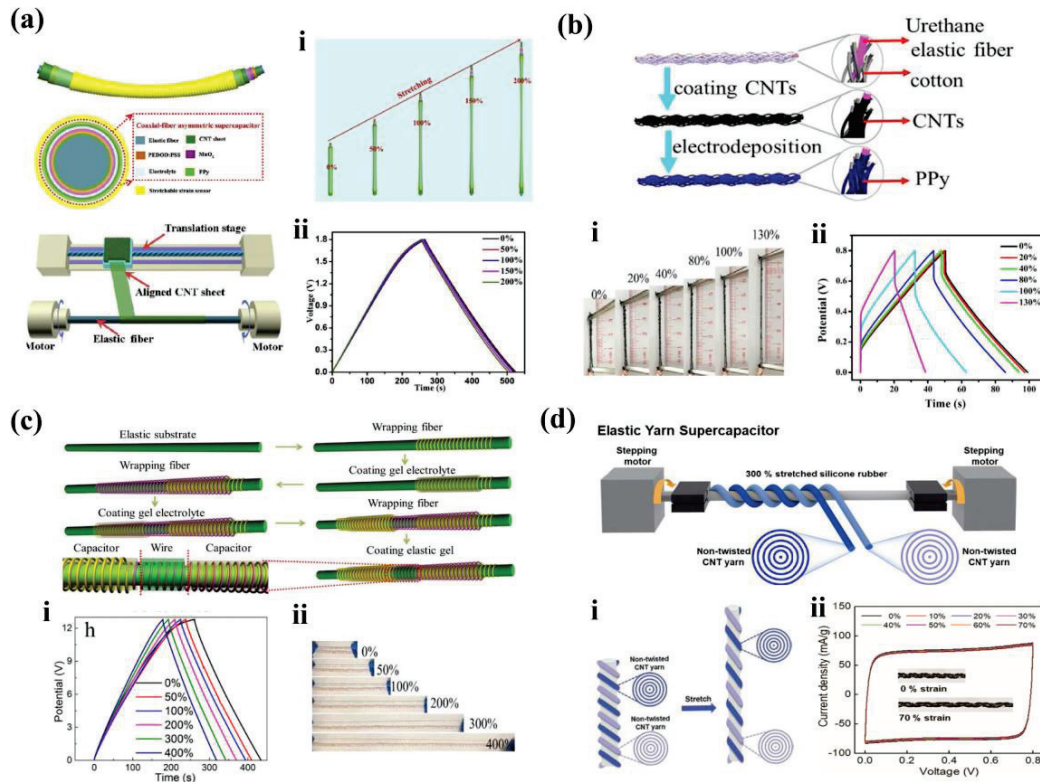


Fig.17 (a) All-in-one stretchable coaxial fiber-shaped SC: i: the diagram of the stretching test, ii: GCD curves at different stretching states. Reproduced with permission ^[140]. Copyright © The Author(s) 2020, Elsevier Ltd. (b) PPy@CNT@urethane fiber based stretchable fiber-shaped SC: i: the diagram of the stretching test, ii: GCD curves at different stretching states. Reproduced with permission ^[141]. Copyright © The Author(s) 2016, Elsevier Ltd. (c) The elastic PEDOT:PSS fiber based helical SC: i: GCD curves at different stretching states, ii: GCD curves at different stretching states. Reproduced with permission ^[141]. Copyright © The Author(s) 2016, Elsevier Ltd. (d) Elastic Yarn Supercapacitor: i: the diagram of the stretching test, ii: GCD curves at different stretching states. Reproduced with permission ^[141]. Copyright © The Author(s) 2016, Elsevier Ltd.

the diagram of the stretching test. Reproduced with permission ^[49]. Copyright © The Author(s) 2018, Elsevier Ltd. (d) Schematic illustration and CV curves of the CNT yarn based helically structured SC: i: the diagram of the stretching state, ii: CV curves at different stretching states. Reproduced with permission ^[142]. Copyright © The Author(s) 2020, Wiley VCH.

4.2.2 Helically Structured Fiber SCs

Carbonaceous and metallic fibers usually have excellent electrical conductivity and chemical stability, but the unpromising elasticity. It is a rational strategy to assemble the fiber-shaped device in a helical or wavy structure for gaining the stretchability. In our previous work, a self-helix fiber-shaped SC was developed with the assist of a stretchable polydimethylsiloxane (PDMS) tube, and the electrochemical performance maintained well even at a high stretching state of 100 % ^[124]. As a typical example, Peng's group fabricated the PEDOT:PSS based elastic fiber as the 1D electrode, which was also used as the conductive wire for connecting a 2 series stretchable SC. As shown in Fig.17.(c), the helical structure was readily obtained by wrapping the 1D electrode onto an elastic substrate back and forth. The resulting helical device demonstrated excellent stretchability without using any additional electrical connections. As a demonstration, a 8 series-connected SC was then prepared, showing a high voltage window of 12.8 V. As it indicated from Fig.17.(c) i and ii, the charging/discharging curves remained well when the strains increased slightly, and a high capacitance retention of 80% was still obtained when the applied strain high to 400 % ^[49]. Very recently, Kim et al. proposed a yarn based energy harvesting and storage one package system. As shown in Fig.17.(d) and inset i, the stepping motor machine was applied for preparing the helically structured electrodes, which was obtained by wrapping the non-twisted CNT yarn parallel around the 300 % stretched silicone rubber fiber. The resulted helical SC was electrochemically measured versus different stretching ranges, as shown the CV curves in Fig.17.(d)-ii, a stable gravimetric capacitance of around $1.5 \text{ F} \cdot \text{g}^{-1}$ was attained under a strain range from 0 % to 70 %. This merit will pave the way for promoting the wearable energy storage

system into applications with more dynamic conditions ^[142].

4.2.3 Knit Fabric SCs

The unique knit structure with the meandering loops endows the textile with high looseness and tensile property. Thus, the knit fabric and knitting technique have the intrinsic advantages in the generating the stretchable SCs. Mai's group reported the strategy of constructing the stretchable SC by using the elastic spandex textile (ST) substrate. As shown in Fig.18, two electroless deposition methods were performed to gain a metallic nickel layer and NiCoP successively. It indicated that NiCoP delivered a very high gravimetric capacitance of about $713 \text{ F} \cdot \text{g}^{-1}$, owing to the strongly adhesion of Ni@NiCoP microparticles with the ST substrate. To understand the reason of the robust combination, the finite element analysis (FEA) was adopted for simulating the surface stress distributions of NiCoP on ST and the normal straight fiber respectively. As shown in Fig.18.(a)-i, the blue and red colors represented the low and high stress respectively, and it reflected that the mechanical stress near the spheres on ST was much lower than that on the straight fiber. Thus, the coiled yarns were theoretically more advantageous for developing a stretchable product. The insets ii and iii of Fig.18.(a) also demonstrated that the SC retained a high capacitance after a stretching test for 1000 cycles at the strain of 40%, and the CV curves kept almost unchanged ^[143].

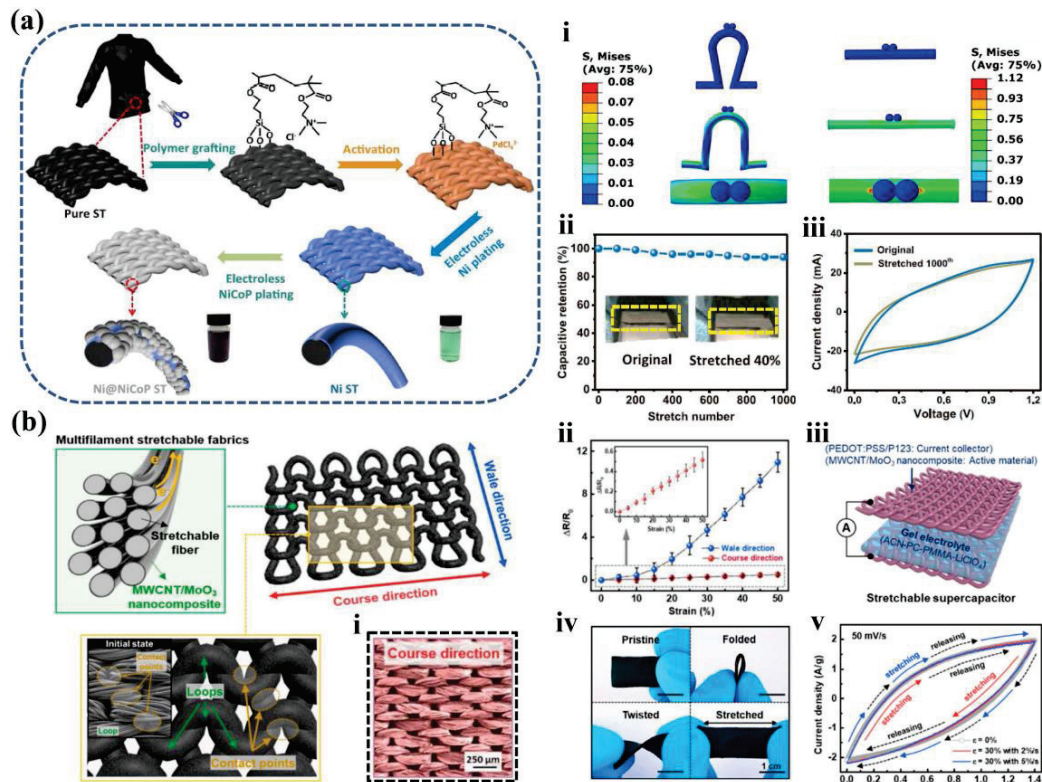


Fig.18 (a) Ni@NiCoP coated spandex textile based SC: i: the finite element analysis, ii: the capacitance retention of 1,000 time of stretching. Reproduced with permission ^[143]. Copyright © The Author(s) 2019, Elsevier Ltd. (b) The stretchable MWCNT/MoO₃ coated knit fabric SC: i: the SEM image of the fabric in the course direction, ii: the relative resistance changes in different directions, iii: the diagram of the SC assembly, iv: the real photos of the device deformations, v: the dynamically recorded CV curves at stretching/releasing states. Reproduced with permission ^[144]. Copyright © The Author(s) 2019, American Chemical Society.

For more in-depth understanding of the knit fabric built stretchable SC, Park et al. studied the changes of resistance in accordance with the applied strain in the course (horizontal loops) and wale (vertical loops) direction. As shown in the diagram of Fig.18.(b) and the SEM image of inset i, the contact points and areas between yarn loops remained well when stretched in the course direction, resulting in a lower resistance increment. By contrast, the relative resistance in wale direction increased by 20-fold higher than that in the course direction, as shown in Fig.18.(b)-ii. Thus, it

was rational to construct the stretchable SC in the course direction of the knit fabric. By constructing the PEDOT:PSS/P123 current collector and multi-walled carbon nanotubes and molybdenum trioxide nanowires (MWCNT/MoO₃) electroactive materials (Fig.18.(b)-iii), the resulted device indicated a volumetric capacitance of 0.41 F·cm⁻³ at a current density of 1.2 mA·cm⁻³. A measurement of the flexibility was then performed in both static and dynamic modes, as demonstrated in Fig.18.(b)-iv, the knit fabric based SC was freely folded, twisted, and stretched. The dynamically recorded CV curves versus different deformation states were also displayed in Fig.18.(b)-v, and the loops recovered nearly the same to the initial state ^[144]. This work demonstrated an in-depth study of using a knit fabric to generate the stretchable SC, and the clear understanding of the resistance changes with the stretch played a key role in realizing the final device.

Apart from the above-mentioned strategies, other fabrics and techniques were also used for developing the stretchable SCs. For example, polyurethanes (PU), which are widely used in textile manufacturing for high-resilience seating, gaskets, etc., are often selected as the elastic substrate for stretchable SCs. Jeong et al. attached the activated carbon (AC) and nanostructured CNTs on the prestretched PU polymer for a highly deformable SC, and no material cracking and destruction occurred at a strain of 100% ^[145]. Wu et al. propose a facile printing method loaded the electroactive materials directly onto the PU textile, resulting in an all-printed stretchable asymmetric SC with the capacitance retention about 86.2% at a strain of 40% ^[146].

4.3 Washability

As the above discussion, textile engineering and technology have enabled SCs with flexibility and stretchability for integrating to the wearable smart system, which also seek for a proper washability in the practical applications. The encapsulation strategy is one of the mostly reported methods that protect both the electroactive materials and

electrolyte from delaminating and leaking by coating an extra specific layer on the outside. In addition, it is also an effective way to directly use the washable materials when constructing the electrode. From the perspective of textiles, the progress of the washable SCs are introduced here, in terms of the fiber-shaped and fabric based substrates. However, the material property and the treatment technique may produce more effects on the washability rather than the textile structure and processing technologies.

4.3.1 Fiber-shaped SCs

Fibers and yarns are the basic units for a textile processing, and it is rational to build up a washable fiber-shaped SC that can be knit or woven into textiles for further applications. As shown in Fig.19.(a), the carbon fibers were electrodeposited with porous FeOOH@PPy and MnO₂, respectively, for an asymmetric solid-state fiber-shaped SC. A high volumetric capacitance of 30.17 F·cm⁻³ was then delivered, and the flexible device was subsequently encapsulated with the Ecoflex polymer for acquiring the washability. As shown in Fig.19.(a)-i, the SEM image of the SC cross indicated that the Ecoflex polymer was uniformly covered on the electrode. Two devices connected in series were then inserted into a common glove, and successfully powered a LED (Fig.19.(a)-ii). For the determination of the washability, the fiber-shaped SC was dipped into a beaker with different solutions (Fig.19.(a)-iii). Considering the practical environment with the sweat or rain drops, the SC was detected in three kinds of solutions, including neutral, acidic, and alkaline mediums. As shown in Fig.19.(a)-iv, the CV curves overlapped very well. The capacitance also retained nearly 100% when subjected to a cycling test in water for 3 h (Fig.19.(a)-v), and it was almost no changes when tested in the stirring water for 8 h. All these consistent results indicated a good polymer encapsulation and great washability^[147].

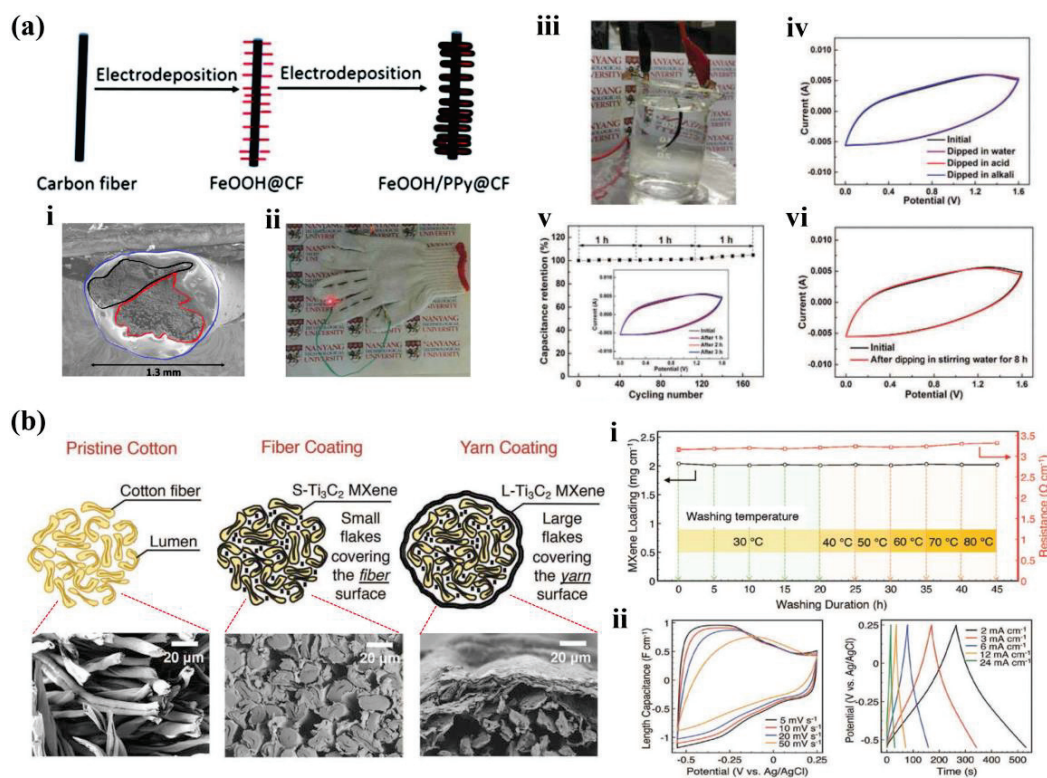


Fig.19 (a) The washable FeOOH@PPy based fiber-shaped SC: i: the SEM image of the SC cross section, ii and iii: the photo of the series SC and the washing method, iv: CV curves in different solutions, v: capacitance retention during the cycling tests 3 h in water, vi: CV curves of the test for 8 h. Reproduced with permission ^[147]. Copyright © The Author(s) 2017, The Royal Society of Chemistry. (b) The fabrication diagram of the MXene flakes encapsulation on the cotton fibers: i: the loading variation and the resistance changes with different washing conditions, ii: CV and GCD curves of the electrode. Reproduced with permission ^[148]. Copyright © The Author(s) 2019, Wiley VCH.

Unlike the strategy of relying on a protective layer, Yury's group reported a washable cellulose yarn by the directly coating of Ti₃C₂T_x MXene flakes. As shown in Fig.20.(b), the cotton yarn was coated twice with the small and large MXene flakes respectively. The small flakes can penetrate into the internal surfaces of the yarn fibers and result in the balanced amount of the electroactive materials, while the large flakes were helpful to the continuous conductivity. With a proper ratio of the two types of MXene flakes, the cellulose yarns with the MXene mass of about 77 wt%

displayed a conductivity of $440 \text{ S}\cdot\text{cm}^{-1}$. The resulted yarns were then washed for 45 times at temperatures from 30 to 80 °C, as shown in Fig.20.(b)-i, the loading mass of MXene almost remained unchanged, while the electrical resistance underwent a slight growth. The CV and GCD curves of the composite yarn based electrode were plotted in Fig.20.(b)-ii, and a length capacitance of $759.5 \text{ mF}\cdot\text{cm}^{-1}$ was achieved at the scanning rate of $2 \text{ mV}\cdot\text{s}^{-1}$. This study provided a novel thought of using the washable materials toward the generation of washable electrode ^[148].

4.3.2 Fabric SCs

As a matter of the fact, the washability of the TWSC is mainly determined by the material intrinsic property and the post-treatment of the device, rather than the textile structures and processing technologies. Therefore, various fabrics were studied for the potentials in gaining a high washability. Wang's group proposed a knitting power textile that combined the energy harvesting and storing systems, and the weft knit fabric demonstrated excellent flexibility and stretchability. The silicone rubber was adopted for gaining the washable TENG, while the carbon nanofiber (CNF) and PEDOT:PSS were directly used for the fabricating the SC electrode, as shown in Fig.20.(a). It was observed that washing can greatly improve the performance of the contaminated device. The photos of contaminated and washed devices are shown in Fig.20.(a)-i. Notably, without any encapsulation, the SC displayed a stable capacitance retention after being washed for 5 times. As shown in Fig.20.(a)-ii and iii, the CV and charging curves of the device before and after washing were nearly overlapped, demonstrating a decent washability of the knit SC ^[50].

Also, Lee et al. used the calligraphic ink decorated the cotton woven fabric resulted the washable SC, without the assistance of the encapsulation layers. Fig.20.(b)-i shows that the sheet resistances of the textile electrode remained well after being washed. From the SEM images in Fig.20.(b)-ii, it can be seen that the surfaces of both the cotton fibers and silver blend fibers had no obvious changes, meaning a robust and

stable adhesion of the ink on the fibers. Moreover, the fabric electrode showed a stable electrical resistance versus the cyclic bending tests before and after wash (Fig.20.(b)-iii), demonstrating both remarkable mechanical flexibility and washability. Based on this, two of the textile electrodes were assembled symmetrically for a washable SC, as shown in Fig.20.(b)-iv, the whole device had a small thickness of about 700 μm . To understand the washability, the GCD curves and capacitance retention were studied versus the washing times. As shown in Fig.20.(b)-v, the calligraphic ink based SC retained nearly 90% capacitance after being washed for 10 times, indicating a great rate capability and washability ^[149].

Screen printing is one of the classic textile techniques. Recent years, it is also widely used in developing the micro SC (MSC), Bonaccorso et al. reported a screen printed MSC based on the ink formulation of aqueous/alcohol graphene and SWCNTs, as shown in Fig.20.(c), the adding of SWCNT can significantly improve the specific area and the conductivity of the interdigital electrodes. The MSC exhibited a power density of above 20 $\text{mW}\cdot\text{cm}^{-2}$ at an energy density of 0.064 $\mu\text{Wh}\cdot\text{cm}^{-2}$. The device was then encapsulated with ethylene vinyl acetate (Fig.20.(c)-i) and washed at the home-laundry conditions for understanding the washability. As shown in Fig.20.(c)-ii, the similar CV and GCD curves were acquired before and after washing, indicating the great waterproof and washable properties ^[150]. Zheng's group proposed an embroidery based washable SC. As shown in Fig.20.(d), a four-letter pattern of "AiMD" was embroidered on a common cotton T-shirt, which were connected in both series and parallel forms. The T-shirt embroidered with the SCs displayed the similar flexibility and softness with the cotton fabric. By encapsulating a waterproof thermoplastic polyurethane (TPU) fabric, both waterproofness and washability were endowed with the T-shirt SC, as shown in Fig.20.(d)-i and ii, the embroidery SC delivered no obvious degradation in the capacitance after being washed for 20 cycles, demonstrating a successful strategy for constructing the textile based washable SC ^[151].

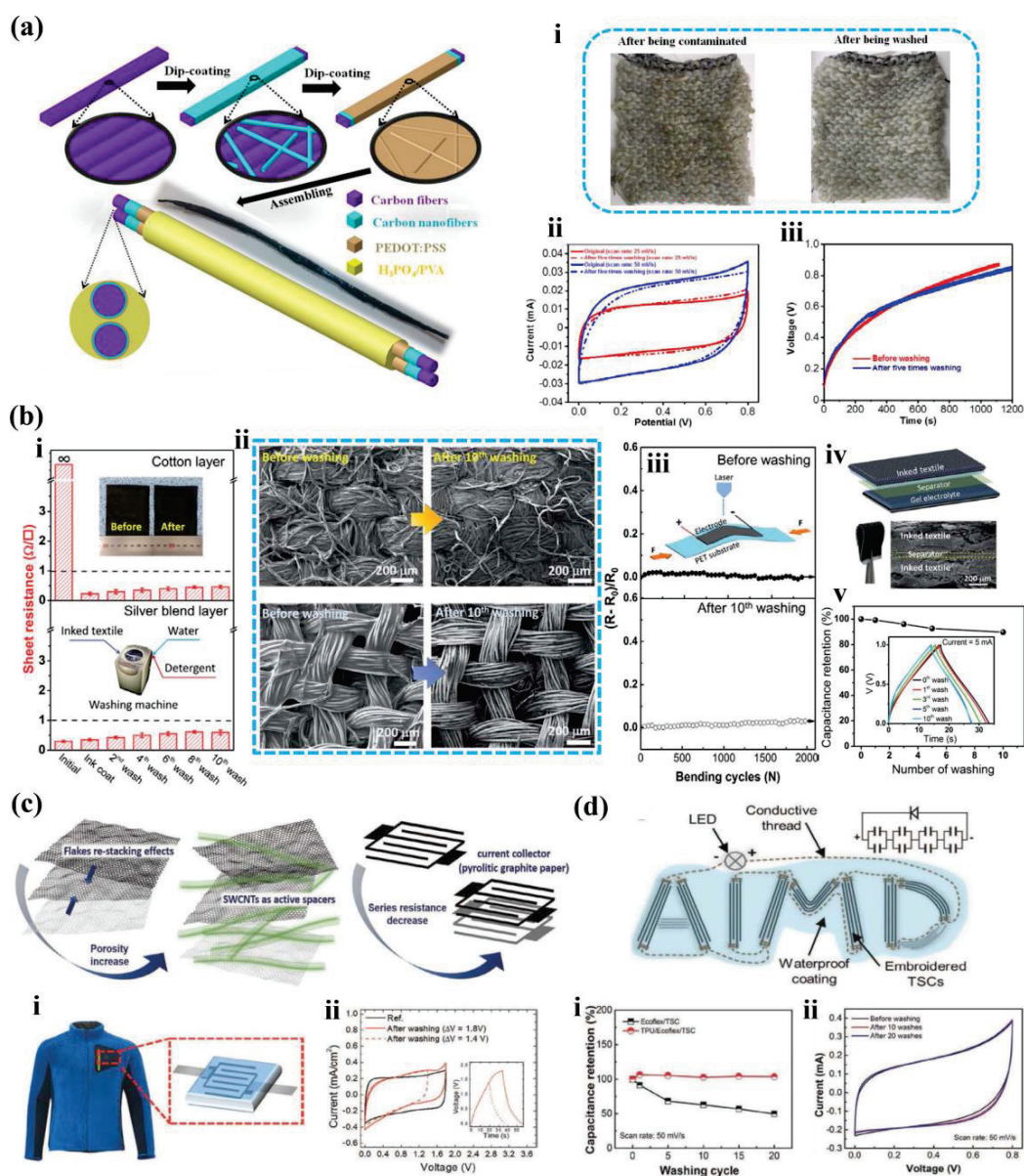


Fig.20 (a) The fabricating diagram of the CNF@PEDOT:PSS knit SC: i: photos of the device before and after washing, ii: CV and charging curves of the SC before and after washing. Reproduced with permission [50]. Copyright © The Author(s) 2017, American Chemical Society. (b) The calligraphic ink decorated woven fabric SC: i: the sheet resistances after different washing times, ii: SEM images of cotton and silver fibers before and after washing, iii: relative resistances at different bending cycles before and after washing, iv: the diagram of the SC, v: capacitance retention at different washing times. Reproduced with permission [149]. Copyright © The Author(s) 2016, The Royal Society of Chemistry. (c) The screen printed washable MSC: i: MSC encapsulated with ethylene vinyl acetate, ii: CV and GCD curves

before and after washing. Reproduced with permission ^[150]. Copyright © The Author(s) 2019, Wiley VCH. (d) The letter patterned embroidery SC: i: the capacitance retention at different washing cycles, ii: CV curves at different washing cycles. Reproduced with permission ^[151]. Copyright © The Author(s) 2020, Wiley VCH.

4.4 Breathability

Breathability, or air permeability, is a basic parameter for textile and garment. From this perspective, the emerging smart textiles and the wearable energy storage devices are required to be evaluated with the characteristic of breathability. Generally, there are two main strategies for endowing a SC with the proper breathability, as shown in Fig.21.(a) ^[152]. The first way is to use the textile techniques, such as the weaving and knitting, to integrate the fiber-shaped SCs into the fabric or garment. Based on the intrinsic feature of the specific textile technique, the resulted textile-based SCs can display a comparable breathability. The second strategy is to directly punch the prepared SC devices with numerous through-holes. Notably, considering the intrinsic poor air permeability of the polymer based electrolyte, the breathability of the fabric electrode is inevitably sacrificed when assembled as the solid-state device, and thus, the punching operation is used for regaining the breathability for the energy storage device. Paper based flexible SCs were then widely developed for acquiring air permeability by the punching treatment ^[152, 153]. Nevertheless, as compared to paper substrates, textile materials usually show much better strength and comfort, and it is thus more advantageous to generate the breathable SCs with the textile based substrates.

Lin et al. selected the highly breathable activated carbon fibers (ACFs) nonwoven veil as the substrate for the SC, as shown in the diagram of Fig.21.(b), the interwined carbon fibers rendered the nonwoven veil tremendous voids and pores, which are the typical conditions for a breathable fabric. By coating with the electrolyte, the ACF veil SC demonstrated a high energy density of $5.52 \text{ Wh}\cdot\text{kg}^{-1}$. The real photo in

Fig.21.(b)-i displayed the nonwoven veil with a typical semitransparent network of

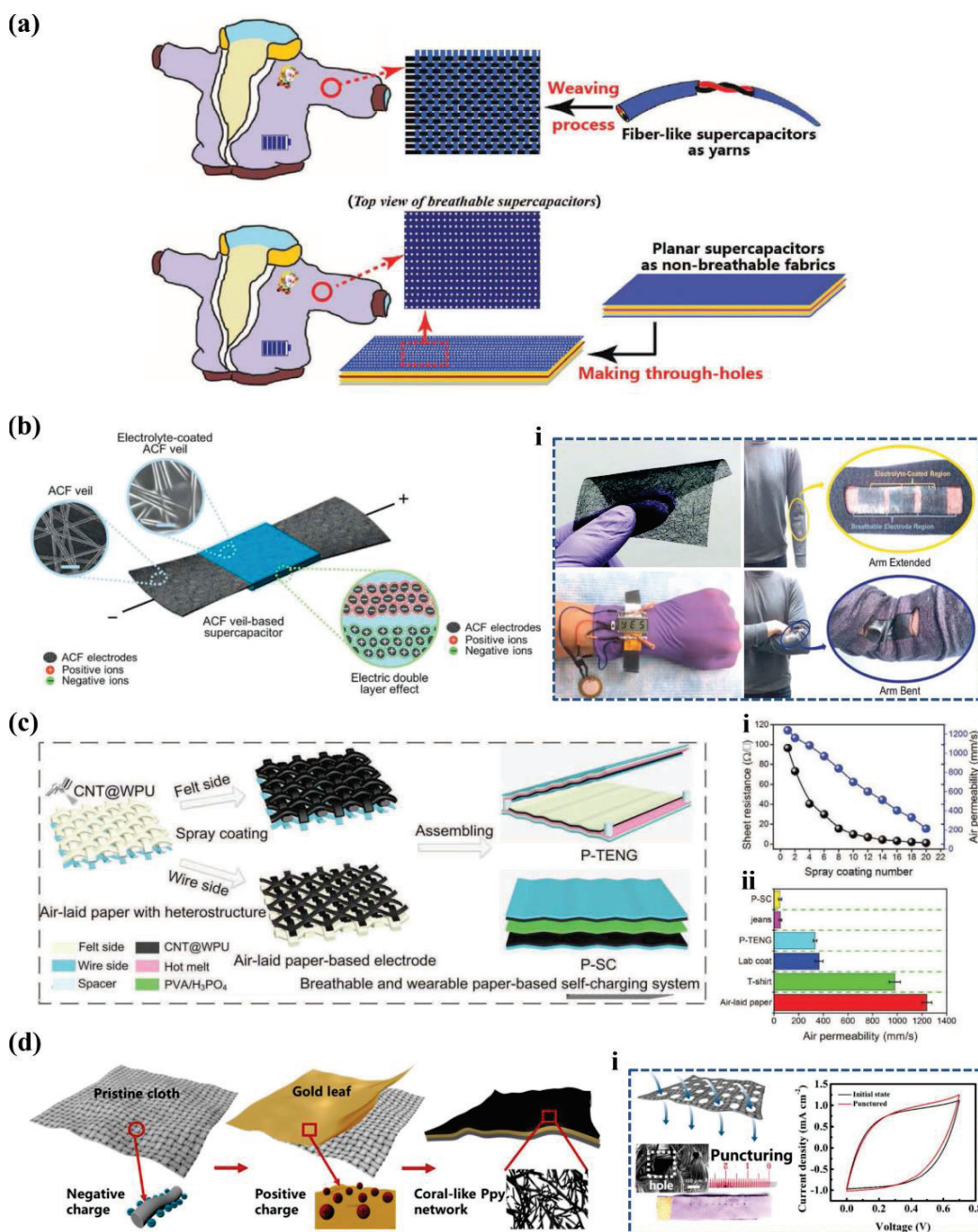


Fig.21 (a) Breathable SC based on highly flexible paper electrodes. Reproduced with permission ^[152]. Copyright © The Author(s) 2016, Wiley VCH. (b) The breathable SC based on ACFs veil: i: the photos of the veil and the derived SC applications. Reproduced with permission ^[154]. Copyright © The Author(s) 2018, Wiley VCH. (c) The air-laid paper based SCs: i: the sheet resistance and air permeability at different coating times, ii: air permeability of different devices and substrates. Reproduced with permission ^[155]. Copyright © The

Author(s) 2019, Wiley VCH. (d) The schematic diagram of the polyester woven cloth based electrode: i: the diagram and CV curve of the punched SC. Reproduced with permission ^[156]. Copyright © The Author(s) 2018, American Chemical Society.

the ACFs, and the SCs connected in series were able to serve as a watchstrap energy storage device for powering an LCD display. For a demonstration, the junction part of the sleeve was substituted by three groups of the series veil SCs. Just as the mentioned before, the solid-state device was not able to be breathable, but the electrolyte uncovered areas displayed the accordant fabric breathability ^[154]. To quantitatively study the breathability, Lu et al. proposed a breathable and wearable self-charging power system consisting of a triboelectric nanogenerator (TENG) and SC. The schematic diagram is shown in the grey box of Fig.21.(c), the air-laid paper with a felt side and wire side was selected for the fabrication of both TENG and SC. By spray coating the composite of MCNT and the waterborne polyurethanes (WPU), the flexible and breathable electrode was prepared. The air permeability of the electrodes fabricated with different spray coating numbers was investigated and plotted in Fig.21.(c)-i, and it indicated that the electrode resulted by 20 times of spray coating showed an air permeability of $214 \text{ mm} \cdot \text{s}^{-1}$, much better than that of the polyvinylidene fluoride (PVDF) based electrode ^[157]. Furthermore, the symmetrically assembled SC was also determined the breathability. Fig.21.(c)-ii demonstrated that the original air-laid paper possessed the highest value of the air permeability, while the resulted SC showed only a limited value of $48 \text{ mm} \cdot \text{s}^{-1}$, due to the presence of the PVA/H₃PO₄ gel electrolyte. Nevertheless, it was still as breathable as the regular jeans ^[155].

To solve the problem of the inferior breathability caused by the electrolyte injection, the strategy of punching holes on the device was gradually implemented. In this way, the fabric structure may have very limited influence on the air permeable property. As shown in Fig.21.(d), the polyester (PET) woven cloth carried negative charges was laminated with the positively charged gold leaf, and a highly conductive and flexible fabric electrode was readily obtained. Subsequently, an electrodeposition was

performed to load the PPy nanorods evenly on the golden PET substrate. The assembled solid-state SC showed an areal capacitance of $17.14 \text{ mF}\cdot\text{cm}^{-2}$ at the current density of $0.2 \text{ mA}\cdot\text{cm}^{-2}$. After the safety evaluation, the punching operation was performed carefully by the needles, as shown in Fig.21.(d)-i, the device was punched with the arrays of small holes, with the diameter around $60 \text{ }\mu\text{m}$. The CV curves of SCs before and after punching were plotted for a comparison, and the almost overlapped CV curves indicated that the punching method is an effective and useful strategy for gaining the breathability without sacrificing the electrochemical properties ^[156].

4.5 Compatibility

To develop a wearable SC as a real product, one of the essential factors is the compatibility, such as the processing compatibility and the product compatibility. Compared to the flexible nontextile substrates like metallic foils and polymer films, TWSCs possess the inherent merits when integrated as an energy storage fabric or garment. In particular, based on the 1D fiber-shaped SCs with great flexibility and adaptability, a wide range of the energy storage products can be derived, and the following context introduces the fabric based SCs derive by textiles and their technologies.

4.5.1 Basic Fabric SCs

Knit, woven, and nonwoven fabrics are three basic common fabrics, which have been widely applied for preparing flexible and wearable energy storage devices. According to the intrinsic textile features and the processing technologies, the TWSCs demonstrate impressive compatibility to the practical garments or other wearables. As discussed before, in 2013, Yury and his group firstly proposed the strategy of using the knitting and weaving methods constructed the flexible SCs, and this work ingeniously displayed the intrinsic advantages of textile substrates and technologies ^[135], initiating a blooming development of the flexible TWSCs.

Knit fabric SCs. To acquire a wearable SC with great compatibility, it is rational to use a knit fabric as the flexible substrate. As discussed before, various nylon and spandex fabrics were applied for gaining the flexibility and stretchability, meanwhile, great compatibility was also obtained ^[143, 144]. By contrast, it is more challenging to achieve a wearable device directly via a knitting technique. Yury's group contributed significantly to this field. After presenting the first knit and woven SCs in 2013, they continued their work by knitting a two-ply yarn (AC-coated yarn and a stainless steel yarn) based stretchable SC, as discussed before in Fig.16.(b), the knit SC was well compatible with the normal fabric, showing a vivid two-in-one effect in clothing processing ^[97]. Very recently, they reported the work of fabricating meters of fiber-shaped electrode for knitting the planar fabric SC. Notably, an industrial yarn coating and knitting technology was successfully applied, as shown in Fig.22.(a). The commercial cotton and nylon yarns in different combinations were fed at a controlled rate through the MXene precursor baths, followed by the drying and winding processes. The resulted functional yarns were then knitted for a planar fabric SC, by the aid of a flat-bed industrial knitting machine (the middle one of Fig.22.(a)). To gain the optimal electrochemical performance, the SC geometry and knitting structure were all studied in details, and it was concluded that the rip structure and interlock stitch were advantageous to build up a high-performance flexible SC. As shown in the image (the right one) of Fig.22.(a), the device delivered a high energy density and power density of $25.41 \text{ Wh}\cdot\text{cm}^{-2}$ and $0.47 \text{ mW}\cdot\text{cm}^{-2}$, respectively. Owing to the one-pot textile processing, the device showed excellent compatibility with the daily garments ^[158].

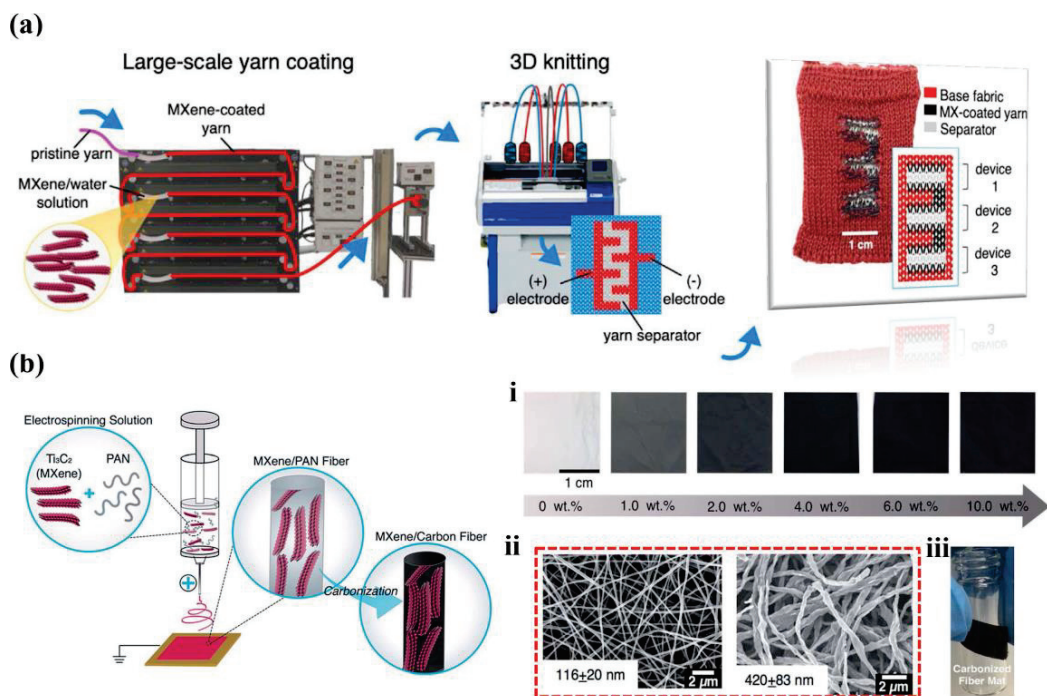


Fig.22 (a) The 3D knit SC using the MXene coated yarns. Reproduced with permission ^[158]. Copyright © The Author(s) 2020, Elsevier Ltd. (b) The electrospun MXene/carbon nanofiber based SC: i: the real photos of mats with various MXene weight percentages, ii: the SEM images of MXene/carbon nanofibers and pure carbon nanofibers carbonized at different temperature, iii: the image of the carbonized mat. Reproduced with permission ^[159]. Copyright © The Author(s) 2019, The Royal Society of Chemistry.

Woven fabric SCs. Similarly, it is also a simple and well-tried strategy to directly functionalize the ready-made woven fabric for a compatible SC. As the previous demonstration in Fig.16.(c), Peng's group reported the functionalized woven fabric based SC, which was able to be extended to as large as 100 cm^2 SC on a T-shirt, demonstrating remarkable compatibility ^[137]. Huang's group proposed the $\text{Cu}(\text{OH})_2$ nanobelt decorated Dacron cloth as the fabric electrode, with a high areal capacitance of $217 \text{ mF} \cdot \text{cm}^{-2}$ at the current density of $0.5 \text{ mA} \cdot \text{cm}^{-2}$. The using of the commercial Dacron cloth set a good example for developing compatible SC from the perspectives of textile substrate ^[52]. In addition, the direct weaving of the flexible SC usually involves more complicated issues, such as the mechanical properties of the fiber-shaped electrodes. As the first report on textile technology based SC, Yury's

group studied and compared the knit fabric SC and woven fabric SC, and it indicated that both of them had great compatibility, with the knit fabric SC showing higher specific capacitance than that of the woven fabric SC. They assumed that the woven fabric SC had lower material loading and conductivity than those of the knit one ^[135]. As discussed in Fig.16.(d), the carbon fiber threads, with the intrinsic high strength and conductivity, were also directly woven as the fabric SC after a hydrophilic treatment, showing a successful compatibility of the SC and fabric processing technology ^[137].

Nonwoven fabric SCs. According to the nonwoven fabric processing, it is a promising strategy to prepare the fabric electrode by directly entangling the electroactive material coated fibers or yarns, which not only shows great electrochemical performance, but also inherent the multiple non-woven textile properties. Yury et al. reported the attempts of fabricating electrospun nanofibers with the composite of MXene flakes and the polyacrylonitrile (PAN), as shown in Fig.22.(b). The non-woven mats were fabricated with varying weight percentages of MXene (Fig.22.(b)-i), with a gradual color deepening upon the MXene ratio from 0 to 10 wt%. After a facile carbonization, the free-standing MXene/carbon nanofibers were achieved, and the SEM images in Fig.22.(b)-ii indicated that an average diameter of 116 ± 20 nm and 420 ± 83 nm was obtained from the pure and 10 wt% MXene@8 wt% PAN fibers, respectively. The work shows a good example for fabricating the high-performance fiber or yarn electrode and the nonwoven fabric electrode, which are compatible to the flexible textile products ^[159].

4.5.2 Sewn and Embroidery SCs

Differing from knitting and weaving which are producing the new fabric, sewing and embroidering is belonging to a decorating tool used for the ready-made fabric. As the advancement of the modern technology, the hand operation of the two techniques have been developed to the automated machine processing ^[160]. By using the sewing

or embroidery technique, the resulted SCs could be intrinsically compatible.

Sewn SCs. There are also two ways can be applied for the sewing technique to construct the flexible SCs. The first one is to fabricate a conductive sewn scaffold, followed by a loading of the electroactive materials. As shown in Fig.23.(a), Lee et al. used the sewing machine and the conductive SSYs created an interdigital stitches as the current collector. A screen printing method was then adopted for loading the electroactive materials of AC and MWCNTs. The resulted solid-state SC displayed a high areal capacitance of $74.2 \text{ mF} \cdot \text{cm}^{-2}$ at a scan rate of $1 \text{ mV} \cdot \text{s}^{-1}$. Based on the sewn SSY route, four groups of the SCs were created in series and parallel respectively on the common fabric, as shown in the left bottom of Fig.23.(a), a quadruple improvement of the voltage (in-series) and the current (in-parallel) was accordingly obtained in the GCD curves. The sewn energy storage device was integrated naturally with the fabric like a logo pattern, embodying the equal property with the normal fabric ^[161]. Another strategy is to sew the fiber-shaped electrode directly. For example, Chen et al. reported a direct sewing strategy for the SC assembly, and the wet-spun rGO electrodes were used as the feeding yarn ^[162], Li et al. also sewed the wet-spun CNT/MnO₂ electrodes into a common fabric directly, and a compatible SC textile was finally achieved ^[163]. In our previous study, the NiCoO₂ covered 1D SSY electrodes were successfully hand-sewn into the cotton fabric, forming a “NiCo” monogrammed fabric ^[47]. In another work, we continued to use the SSY yarns, and fabricated the 1D fiber-shaped rGO@SSY//NiCo₂S₄@SSY SC, as shown in Fig.23.(b), the fiber-shaped SC can be hand-sewn into various monogrammed patterns, such as the “PolyU” and “ITC”, demonstrating excellent features in both compatible processing and products ^[124].

Embroidery SCs. Similar to the sewing technique, the modern technology has also promoted the conventional hand embroidering to a more accurate and controllable computerized programming. As a long-standing textile technology, an embroidery product normally shows the inherent textile compatibility. For the machining process,

the embroidering subjects the fiber-shaped electrodes to the harsh mechanical deformation ^[151]. Also, the construction of embroidery SC includes functionalizing the substrate fabric and embroidering the SC yarn. In our previous work, for the first time, the conductive embroidery with an interdigital pattern was built up on a normal fabric as the current collector, as shown in Fig.23.(c), the silver-plated nylon yarns (SPNYs) served as the feeding yarn of the industrial embroidering machine, forming a well controlled current collector pattern. By loading the electroactive material of CoP, the embroidery SC showed an areal capacitance of $156.6 \text{ mF}\cdot\text{cm}^{-2}$ at the current density of $0.6 \text{ mA}\cdot\text{cm}^{-2}$. To demonstrate the processing compatibility and the scalable productivity, a monogrammed pattern “PolyU” was then embroidered on the lab gown, resulting in a novel prototype of the wearable embroidery SC ^[51]. Another strategy is to use the flexible electrode embroider the fabric device. For example, Zheng’s group reported a strategy of additive functionalization and embroidery manufacturing (AFEM). As shown in Fig.23.(d), the rGO@Ni coated cotton yarns were properly embroidered on the fabric and fastened by the insulating fixing yarns. To optimize the embroidery SC performance, they compared two SC structures with different embroidering routes, including the in-plane TSCs (the laterally interdigital structure) and out-of-plane TSCs (the vertically stacked structure). The electrochemical measurement indicated that the shorter electrode spacing of the out-of-plane TSC rendered a smaller IR drop and higher areal capacitance than that of the in-plane TSC. In doing so, a group of SCs were then created on a practical T-shirt, as shown in the bottom of Fig.23.(d), very high capacitance retentions were obtained even at severe deformations, indicating outstanding compatibility between the fiber-shaped electrode and the embroidery SC ^[151].

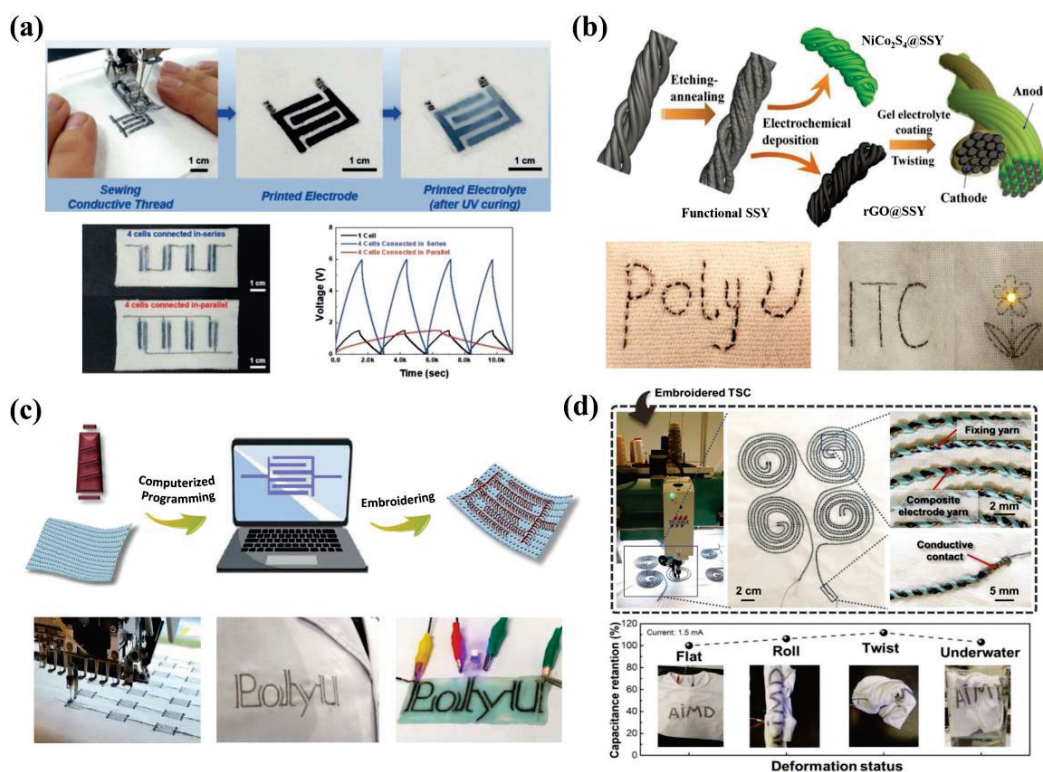


Fig.23 (a) The sewing-printing fabrication for wearable SCs. Reproduced with permission ^[161]. Copyright © The Author(s) 2018, Wiley VCH. (b) The diagram and photos of the hand sewn fiber-shaped SC. Reproduced with permission ^[124]. Copyright © The Author(s) 2018, Wiley VCH. (c) Sketch of the computerized-programming embroidering and the real photos of the embroidery SC. Reproduced with permission ^[51]. Copyright © The Author(s) 2019, Springer Nature Switzerland AG. (d) The schematic photos of the embroidered SC and the flexibility test. Reproduced with permission ^[151]. Copyright © The Author(s) 2020, Wiley VCH.

4.5.3 3DSF SCs

As introduced in sec.3.3.7, the 3D spacing fabric is a unique product in textile industry. Coincidentally, it has almost the same structure with the electrochemical storage device. Inspired by the structure similarity and processing compatibility, our group, for the first time, applied the flat-bed knitting machine fabricated the conductive 3DSF frame, as shown in Fig.24.(a), the SPNYs were used for knitting the top and bottom conductive layers, while the polyester yarns were adopted as the inlay and connecting yarns. Based on the conductive 3DSF frame, MnO_2 and reduced

graphene oxide (ErGO) were electrodeposited as the positive and negative electrode, respectively (Fig.24.(b)). To maintain a stable electrochemical property, an additional layer of the metallic Ni pre-covered on the SPNYs. The SEM images in Fig.24.(c) showed a typical sandwiched SC structure, and the electroactive materials were well coated on the conductive yarns. For the purpose of gaining a real product, the device was then packaged by a multifunctional polyurethane (PU) based hot stamping process, as shown in Fig.24.(d), the 3DSF SC had a large voltage window (1.3 V), with a high areal capacitance of about $1.02 \text{ F} \cdot \text{cm}^{-2}$. By connecting two devices in series, a LED was successfully lit up. Notably, owing to the strong PU protecting layer, the device was performed an abrasion test referring to the ASTM D 3512 method, and the capacitance retained well after 100 times of the abrasion, displaying remarkable wear resistances [164].

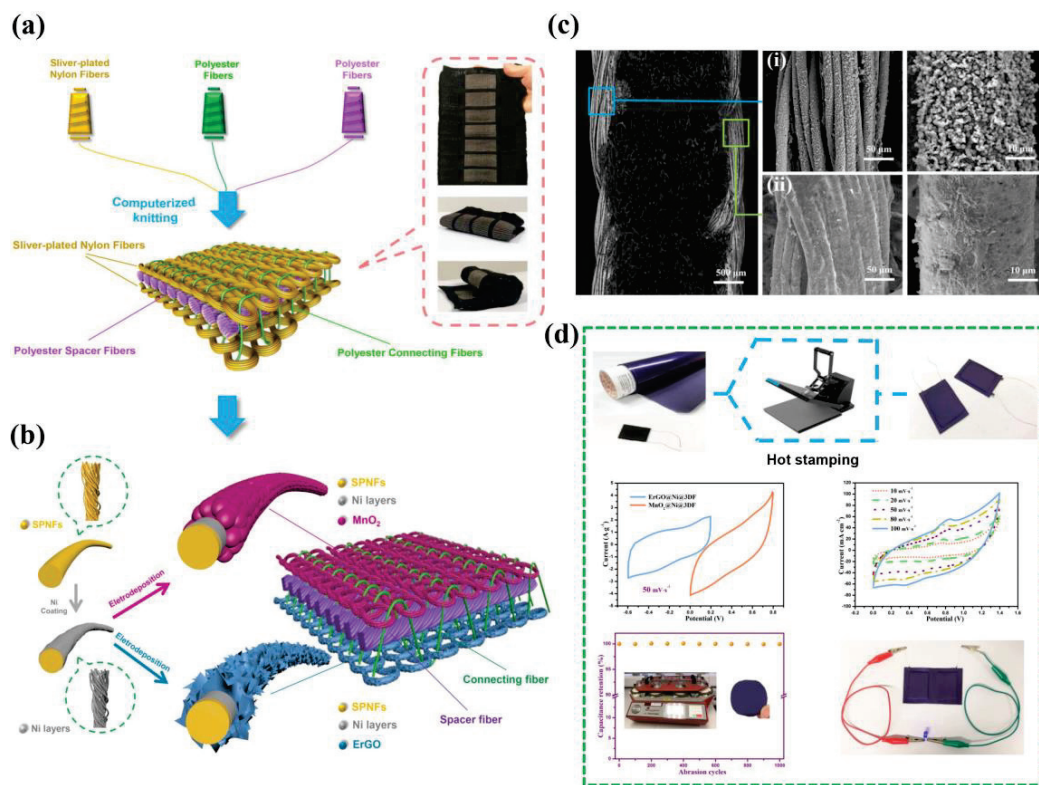


Fig.24 (a) the schematic diagram of the 3DSF SC frame, (b) the fabricating diagram of the 3DSF SC, (c) the SEM images of the MnO₂@Ni and ErGO@Ni electrodes, (d) the PU encapsulation sketch, CV curves and the abrasion test of the encapsulated device. Reproduced with permission [164]. Copyright © The Author(s) 2020, Elsevier Ltd.

4.6 Electrochemical performance

In addition to the above discussion on the unique features of TWSCs, Table 1 summarized the detailed electrochemical properties of the recently reported TWSCs, which are displayed by the device type, configuration, capacitance, energy and power density, cycling life, and the flexibility. Even if, it is still hard to fully compare the device property relying only on the listed parameters, because most of them were measured and calculated under different experimental conditions and metrics ^[165]. Therefore, table 1 provides a summary of the analogous works, intuitively demonstrating the significant achievements from the related works, inspiring the readers have an overall understanding about the TWSCs.

Table 1. Comparison of the electrochemical property of TWSCs in different types

Device type	Configuration (Negative/Positive)	Capacitance	Energy density	Power density	Cycle life	Flexibility
Yarn core-sheath	PPy@SSY // NiCoO ₂ @SSY ^[47]	14.69 F·cm ⁻³	3.83 mWh·cm ⁻³	18.75 mW·cm ⁻³	95% @ 6,000th	95% @180° bending
Yarn core-sheath	rGO@SSY // NiCo ₂ S ₄ @SSY ^[124]	127.2 mF·cm ⁻²	10.19 mWh·cm ⁻³	121.9 mW·cm ⁻³	86.2% @ 3,000th	95% @knotting
Yarn core-sheath	PANI@CFT // FCFT ^[166]	4.8 F·cm ⁻³	2 mWh·cm ⁻³	11 W·cm ⁻³	81% @ 10,000th	Well maintained @stretching 100%
Yarn core-sheath	CoNiO ₂ @CF// AC@CF ^[125]	795.4 F·g ⁻¹	0.95 mWh·cm ⁻³	1.14 mW·cm ⁻³	97% @ 5,000th	No attenuation @bending 500th
Yarn core-sheath	EACF// CoSe ₂ @PPy ^[167]	226 mF·cm ⁻²	0.87 mWh·cm ⁻³	0.13 W·cm ⁻³	80.1% @ 15,000th	99.3% @180° bending
Yarn core-sheath	NiO@CNTs@CuO@Cu// AC@CF ^[168]	230.48 mAh·g	26.32 Wh·kg ⁻¹	1218.33 W·kg ⁻¹	83.6% @ 2,000th	98.9% @ various positions
Yarn core-sheath	VN// ZnCoO ₂ /CNTF ^[169]	150 mF·cm ⁻²	17.78 mWh·cm ⁻³	80 mW·cm ⁻³	-	Remain 91% @ bending 3000
Yarn Integration	rGO hydrogel symmetric ^[170]	148 F·cm ⁻³	8.8 mWh·cm ⁻³	30.77 mW·cm ⁻³	86% @ 17,000th	CV little changes @ various shape

Yarn Integration	MXene@CNTs// RuO ₂ @CNTs ^[127]	554 mF·cm ⁻²	168 μWh·cm ⁻²	14.8 μW·cm ⁻²	90% @ 10,000th	Near 100% @ bending 1000th
Yarn Integration	SWCNT// MnO ₂ /SWCNT ^[163]	74.8 F·cm ⁻³	10.4 mWh·cm ⁻³	0.05 W·cm ⁻³	94% @ 5,000th	Negligible decrease@ different bending
Yarn Integration	rGO@PEDOT:PSS symmetric ^[171]	131 mF·cm ⁻²	4.55 μWh·cm ⁻²	125 μW·cm ⁻²	80% @ 1,800th	Remain well@180° bending
Yarn Integration	PEDOT: PSS symmetric ^[49]	93.1 mF·cm ⁻²	8.3 μWh·cm ⁻²	400 μW·cm ⁻²	89% @ 5,000th	Unchanged CV @bending 2,000th
Coaxial structure	VN@CNTs// MnO ₂ @CNTs ^[126]	213.5 mF·cm ⁻²	96.07 μWh·cm ⁻²	270 μW·cm ⁻²	90% @ 6,000th	96.8% @bending 5,000th
Coaxial structure	rGO//rGO ^[172]	205 mF·cm ⁻²	17.5 μWh·cm ⁻²	815 μW·cm ⁻²	100% @ 10,000th	92%@bending 100th
Coaxial structure	NiCo ₂ O ₄ /@Ni wire symmetric ^[173]	10.3 F·cm ⁻³	1.44 mWh·cm ⁻³	17 W·cm ⁻³	78% @ 5,000th	90%@bending 500th
Coaxial structure	MnO ₂ @CNT/G@Ni symmetric ^[174]	31 mF·cm ⁻²	3.1 μWh·cm ⁻²	120 μW·cm ⁻²	82% @ 10,000th	-
Coaxial structure	AC// MnNiCo-CH@CF ^[175]	96.13 F·g ⁻¹	30.04 Wh·kg ⁻¹	749.97 W·kg ⁻¹	83.86% @ 8,000th	no obvious deterioration after bending
Knit Fabric	Ni@NiCoP@SWCNT// Ni@NiCoP ^[143]	171.4 mF·cm ⁻²	-	-	98% @ 6,000th	100%@after bending
Knit Fabric	PPy@CNTFFs electrode ^[176]	4734 mF·cm ⁻²	-	-	90% @ 5,000th	-
Knit Polyester Fabric	AC@CF ^[177]	0.51 F·cm ⁻²	-	-	-	80%@after bending
Knit Fabric	PEDOT symmetric ^[178]	0.64 F·cm ⁻²	-	-	Unchanged@ 5,000th	100%@after straining
Knit	MoO ₃ /PEDOT/MWCNT	33.8	13.15	100	76% @	100%@after straining

Fabric	symmetric ^[144]	mF·cm ⁻²	Wh·kg ⁻¹	W·kg ⁻¹	10,000th	
Woven Fabric	ACFT// TiN@MnO ₂ ^[179]	1.2 F·cm ⁻²	4.7 mWh·cm ⁻³	2 W·cm ⁻³	89.5% 30,000th	Unchanged CV after bending
Woven spandex fabric	VPPyNTs/CNOs@PPyG symmetric ^[180]	64 F·g ⁻¹	5.7 Wh·kg ⁻¹	-	85% 1,000th	99%@stretching 500 cycles
Woven polyester fabric	GNP symmetric ^[181]	26 pF·cm ⁻²	-	-	-	96%@bending radius (1-3 cm)
Woven ATC fabric	CS//CS-CoNi ^[182]	284 mF·cm ⁻²	1.4 mWh·cm ⁻³	24 mW·cm ⁻³	93% 45,000th	Nearly identical@135° bending
Woven cotton fabric	Ni/MnO ₂ /rGO symmetric ^[134]	412 mF·cm ⁻²	65 μWh·cm ⁻²	0.4 mW·cm ⁻²	89.6% 3,000th	almost without distortion@deformations
Woven cotton fabric	Cu-MOF@CC electrode ^[183]	1812 mF·cm ⁻²	3.14 mWh·cm ⁻³	6.24 mW·cm ⁻³	90% 2,000th	-
Woven polyester fabric	PANI/CNTs/G/PETC electrode ^[184]	791 mF·cm ⁻²	-	-	76% 3,000th	83%@twisting 500th
Nonwoven fabric	MnO ₂ @AuNF symmetric ^[185]	8.26 mF·cm ⁻²	0.14 μWh·cm ⁻²	4 μW·cm ⁻²	94% 10,000th	93%@bending 10,000th
Nonwoven fabric	AC@CNT symmetric ^[145]	128 F·g ⁻¹ (electrode)	≈6 Wh·kg ⁻¹	≈90 W·kg ⁻¹	100% 1,000th	Identical@bending
Nonwoven fabric	NiCoSe ₂ @PPy@GF symmetric ^[186]	5.21 F·cm ⁻³	1.09 mWh·cm ⁻³	16.5 mW·cm ⁻³	82% 5,000th	No significant change after bending 200th
Nonwoven fabric	HN-CNFs@GNs symmetric ^[187]	249 F·g ⁻¹	6.3 Wh·kg ⁻¹	344.1 W·kg ⁻¹	99% 5,000th	No obvious decay @ bending 180°
Nonwoven SC	PP@GO symmetric ^[188]	4.18 mF·cm ⁻²	0.58 μWh·cm ⁻²	14.1 mW·cm ⁻²	-	-
Ink printing	Ni@MnO ₂ @Au-Ag interdigital ^[189]	52.9 mF·cm ⁻²	11.1 mWh·cm ⁻³	39.6 mW·cm ⁻³	80% 5,000th	77.4%@bending 500th

Screen printing	MnO ₂ @CNT-PEDOT interdigital ^[189]	180 mF·cm ⁻²	17.5 mWh·cm ⁻²	0.4 mW·cm ⁻²	A slight increase@ 500th	95.26%@stretching by 20%
Screen printing	FeOOH@MnO ₂ interdigital ^[190]	5.7 mF·cm ⁻²	0.5 μWh·cm ⁻²	40 μW·cm ⁻²	80%@ 2,000th	-
Screen printing	MnO ₂ @Carbon symmetric ^[191]	19.23 mF·cm ⁻²	0.5 μWh·cm ⁻²	40 μW·cm ⁻²	84%@ 2,000th	No structure changes@bending 100th
Screen printing	NiCo ₂ O ₄ symmetric ^[192]	3.45 mF·cm ⁻²	1.77 μWh·cm ⁻²	≈0.3 mW·cm ⁻²	90.95%@ 5,000th	94.2%@bending 200th
Embroidery	CoP@Ni@Ag wire Interdigital ^[189]	156.6 mF·cm ⁻²	0.013 mWh·cm ⁻²	0.24 mW·cm ⁻²	95%@ 5,000th	No obvious decay @bending 200th
Embroidery	ERGO@Ni-Cotton symmetric ^[151]	10.38 mF·cm ⁻²	0.57 μWh·cm ⁻²	2.4 mW·cm ⁻²	94%@ 4,000th	Remain stable @35% stretching
3DSF	rGO@Ni@Ag// MnO ₂ @Ni@Ag ^[164]	1.02 F·cm ⁻²	1.02 mWh·cm ⁻²	5.27 mW·cm ⁻²	85.2%@ 5,000th	94.52%@bending 100th

5 Strategies for Performance Improvement of TWSCs

Although advantages have been highlighted in the above section, challenges still remain to be solved, which include issues of unsatisfied electrochemical performance, ineffective wearability, less end products, etc. ^[148, 158, 193]. Based on the textile substrates and wearable technologies, this section proposes the potential solutions for the main difficulties, from the viewpoints of electroactive material, functional materials, and textile technologies.

5.1 Mass Increase of Electroactive Material for Better Energy Supply

For a SC, the electroactive material loading tends to be lower for gaining higher specific performances (eg: gravimetric capacitance, power density), due to the unique fast charge-storage mechanism of the ion adsorption/dsorption on or near the surfaces.

However, this is unreasonable for developing flexible SC when considering the energy requirement from the practical application, which is estimated to need about 100- μm thick of the electroactive material [30, 32, 33, 194]. Thus, it is a significant direction to enable flexible SCs with higher loading masses of the electroactive materials. Considering the constructing approaches for a TWSC electrode, the mass increasing strategies are discussed following the category of functionalizing the textile and directly fabricating textile electrode.

5.1.1 Functionalized Textile

It is a common strategy to cover the electroactive material on a ready-made fabric for gaining the wearable electrode, which also involves a conductive treatment for a current collector, and the whole treatments are applying the strategy of functionalizing the textile. To improve the electroactive material mass, it is not only about the direct increase of the mass, but also lies in the suppression of the electroactive material delamination.

Using conductive electroactive materials. Considering the general electrode fabrications referring to the conductive and capacitive layers, it should be given preference to the highly conductive electroactive materials which can also serve as the current collector. As proposed by Yury's group in Fig.20.(b)), MXene flakes with great conductivity was coated onto the cotton yarns. By applying MXene flakes in different sizes, both the internal and external surfaces of the cotton yarns were well covered, displaying the continuous conductivity in a wide dimension range. Based on that, a high mass loading MXene flakes were achieved on the cotton yarns [148].

Engineering porous nanostructures. As the major pseudocapacitive materials showed poor conductivity, it is necessary to find new paths to improve the loading. Inspired by the mechanism of the nanostructured battery materials that indicate capacitor-like properties [195], such as LiCoO_2 , it is also a rational strategy for the

intrinsically capacitive material to be engineered in a nanostructured form. Taking the typical example of manganese oxide that bears very high specific capacitance but low conductivity, Liu et al. successfully electrodeposited the porous MnO_x onto the carbon cloth by adjusting the complexing agent concentration in the plating solution, and the resulted electrode showed a high MnO_x mass loading of $7.02 \text{ mg}\cdot\text{cm}^{-2}$, with remarkable specific capacitance and rate capability. Both of the mass and performance were much higher than those of the peer works ^[196]. Also, Kim et al. proposed a work of using the alternating depositions to load MnO_2 and Ag layers on the commercially CNT yarns. The resulted interconnected networks provided better electrical contact between MnO_2 layers with the assist of Ag layer, which shortened the charge and ion diffusion distances ^[197].

Adopting novel electrode preparations. Although thick electrodes can be optimized via the nanostructured engineering, serious aggregation could be occurred at the same time, leading to the poor electrical and ionic transport ^[198-200]. Thus, focus should also be put onto the novel electrode preparations. The characteristics of the textile substrate usually play key roles in determining the load mass and even the electrochemical performance of the functionalized electrode. At the early stage of the textile electrode studies, Yury's group had compared the SC electrode fabricated on the knit and woven fabric respectively, and pointed out that the knit fabric electrode had better areal capacitance than the woven one, because of the higher mass loading of the electroactive material onto the knit fabric. As compared to the woven fabric, knit fabric processed with the intermeshes loops shows higher specific surface areas ^[135]. In this regards, choosing textile substrate is also effective to increase the electroactive material loadings of the electrode.

In addition to the selection of the substrate, it is also essential to apply novel coating method for the electrode preparation, rather than relying only on the conventional carbon slurry based coating technique. For instance, Zheng's group developed a brand new strategy to overcome the rigid caused by thick material as well as low mass

loading of the electroactive materials. By applying the soft hybrid scaffold (SHS) via a simple vacuum filtration process, the thicker nonwoven textile electrode was obtained by using pseudo-materials anchored carbon nanotubes (CNTs) and reduced holey graphene oxides (rHGOs). In doing so, the conductive 3D framework successfully overcame the aggregation and poor conductivity flaws, and the electrochemical performance was highly improved than the conventional preparations, and even exceeded the commercial SC ^[201].

Suppressing material delamination. Apart from the efforts on constructing thick electroactive materials, it is a complementary way to find methods to suppress the material delaminating from the substrate. In our previous work, we adopted SSY as the fiber-shaped electrode substrate, suffering from the cobalt hydroxides delaminating. By treating the smooth SSY surfaces with the strong acid solution, the resulted electrode showed an enhanced adhesion between the electroactive materials and the SSY ^[47, 124]. Moreover, fabricating the composite materials is also an effective way to reduce the delaminating phenomenon. For example, Hu's group coated a layer of PPy onto CNT decorated cotton yarns, and acquired a highly stretchable composite yarn electrode ^[141]; Han et al. covered PPy on MnO₂ nanoparticles anchored CNT textile, and successfully prevented the delamination of MnO₂ ^[202].

5.1.2 Textile Electrode

Due to the limited loading mass and poor adhesion of the electroactive materials on the fabric substrate, the one-pot fabrication of textile electrode is also popular with the researchers, which involves the use of the mixture of the electroactive and supporting materials. Nevertheless, there is also much room in the loading amount and morphology structure of the electroactive material, corresponding to the strategies of increasing the electroactive material ratio and optimizing the internal percolating networks.

Using conductive electroactive materials. As the same to the strategy proposed in functionalized textile, enclosing more conductive electroactive materials in the preparation is also essential. Typically, carbon-based materials are widely used for the EDLC device, owing to the large specific surface areas, high conductivity and the excellent chemical and mechanical stability. It is rational to adopt different carbon-based materials in the preparation of the textile electrode. Besides, to further improve the energy density of the device, it is also necessary to apply more pseudocapacitive materials during the one-pot electrode fabrication. One of the successful used one is MXene, which had shown unique merits in hydrophilicity, electrical conductivity, etc. [203]. Yury's group performed plenty of works on the application of MXene into the energy storage field [148, 203-205], as introduced in the former section, and they successfully applied an electrospinning method for fabricating the 1D integrated electrode. By combining CNTs sheets with MXene, the resulted asymmetric SC demonstrated remarkable energy density [127].

Fabricating electrode without additives. For the one-pot textile electrode, especially the integrated yarn or fiber electrode, fabrication is usually performed with the assist of the polymer based binding materials or other additives, which can pose negative effects on both the electrochemical and mechanical properties. Thus, it is of importance to choose novel method by reducing the use of the irrelative materials. For example, as discussed in Fig.22.(b), MXene flakes were well dispersed in PAN solutions in the spinning dope without any additives, and the MXene@C non-woven mat was then successfully achieved via the electrospinning and annealing processes. By adjusting the ratio of MXene to PAN, the resulted mats showed a high MXene weight percentage up to 35 wt%, providing a promising strategy for developing highly loaded textile electrode [148].

Applying textile techniques. For the textile electrode, it is reasonable and efficient to incorporate the electroactive materials into the fabrication of the textile manufacturing process. A couple of works have demonstrated the successful examples of fabricating

the fiber-shaped electrode or coaxial SCs ^[126, 140]. Taking the yarn electrode preparation as an example, CNT fibers were properly modified by covering a layer of the CNT sheets via the motor assisted yarn twisting method, in order to gain the CNT yarns with both high electrochemical and mechanical properties,. By repeating the twisting process, the electrodes with different CNT sheet thicknesses were readily achieved ^[126]. To construct the coaxial SC device, it is useful to apply the motor based equipment to fabricate the outer shell-electrode, as mentioned in Fig.15(b), and CNT sheets were uniformly wrapped onto the electrolyte coated inner electrode for as the outer tubular electrode ^[126]. As we discussed before, the similar strategies have been also applied in fabricating the elastic yarns, which needed a helical structure ^[141].

In addition to the yarn fabrication, using different textile techniques can bring about novel features for the fabric electrode. As introduced in Fig.22.(a), the authors studied both knit device geometry and structure to optimize the overall performance of the knit SC. For the knit geometry, the influences of length/width of electrodes and the spacing distance between electrodes were studied in details, and for the knit structure, both the rib and jersey structures were prepared via half-gauge and interlock stitch patterns, respectively. It concluded that, for a certain device, the geometry and structure differences result in different loading mass of the electroactive materials. After the comparisons of performance obtained at different parameters, the MXene coated yarns knit SC with the optimal performance was successfully achieved ^[158].

5.2 Unique Material for Multifunctional TWSC

Owing to the textiles and their manufacturing technologies, various functions have been endowed to TWSC, including the above-mentioned stretchability, washability, breathability, compatibility, etc. Nevertheless, the current research status is still far from enough to gain the practical-level functional SC products. There are still works needing to be placed on the perspective of the functional materials.

5.2.1 Functional Electroactive Material

In addition to provide high performance in capacitance, electroactive materials are also expected to be bearing the corresponding functions of the device, like the stretchability, washability, etc.. In doing so, the electrode structures and fabrication process are able to be simplified and highly efficient. The typical features of the electroactive materials other than the electrochemical properties are listed as below.

Using the stretchable electroactive materials. Although a large number of the stretchable SCs have been reported, the loaded electroactive materials were not always stretchable, and they were under the risk of delaminating from the substrate when strained. Therefore, it is significant for the electroactive materials to be bearing with comparable stretchability with the other components. Lv et al. demonstrated an exemplified work to fabricate the stretchable planar fabric device. At first, they printed a layer of the soft styrene ethylene butylene styrene block copolymer (SEBS) elastomer onto the fabric, in order to build the substrate for the following stretchable Ag ink based current collector layer. By incorporating the elastic PEDOT:PSS and PU into the electroactive material stock ink made up of MnO_2 -CNTs and COOH -CNTs, the screen printed fabric electrode displayed excellent stretchability, without sacrificing the capacitance ^[206].

Applying the washable electroactive materials. If an electroactive material had a certain degree of the washability, the extra washable materials would be less or excluded for use. Thus, it is a novel strategy to apply the washable electroactive materials when fabricating TWSC. As introduced in Fig.20.(b), Lee et al. used the conventional calligraphic ink decorated the cotton woven fabric without any encapsulation layers, and the resulted electrode displayed robust and stable adhesion with the substrate fibers, demonstrating impressive washability ^[149]. This work provides the inspirations to pay attention to new route of finding functional electroactive materials.

Adopting the wear-resistant electroactive materials. To process a textile electrode via the textile manufacturing technique, it is a critical parameter for the electrode to have proper wear resistance. Although it is rational to couple the electrode with a protective layer, it may cause some negative effects, such as the poor ion and electron transport. Thus, it is much better to use a wear-resistant electroactive material directly. As per the work presented by Yury's group, the cotton and nylon yarns were successfully covered with the MXene flakes via the industrialized coating process, without using any protective layer, and the resulted functional yarns were directly knitted for a planar fabric SC, demonstrating excellent the practical-level wear-resistance ^[158].

Apart from the above-mentioned typical functions of the wearable TWSCs, there are various other properties waiting for further investigations, and the electroactive materials with other functions are highly expected. For example, Dong's group proposed the novel organic dyes spray-coated fabric electrode via the conventional dyeing process to improve the capacitance performance of the fabric, providing a good example to develop high performance TWSC ^[207].

5.2.2 Stretchable and Robust Solid-state Electrolyte

In views of the fabric substrates and electroactive materials, substantial works have been presented, but the influences of the electrolyte on the device properties were rarely reported. Several features, such as the stretchability and robustness, should be qualified to meet the requirement from the multifunctional TWSC. As a basic characteristic of the wearable energy storage device, the stretchability is significant for the electrolyte to support the whole flexible device. PVA has been widely used in assembling the all-solid-state TWSC, but it could be broken when strained at a large range ^[208]. To maintain the comparable electrochemical performance, the substitute materials for PVA are rather rare. As proposed by Zhi's group, the polyacrylamide (PAM) based electrolyte demonstrated great potential in the application of the

aqueous energy storage system, including the SC and the zinc-ion battery. The PAM electrolyte has the intrinsic stretchability and compressibility, providing an effective solution to the multifunctional TWSC. Also, owing to the ultrahigh stretchability, the PAM can withstand very large strains, indicating an improved mechanical property [209, 210].

Other properties like the breathability and compatibility are also expected to be developed. In particular, it is a dilemma to use the gel-state electrolyte to assemble the breathable electrode for a SC device. Very similarly, when a textile based electrode was used for the device assembly by the gel-state electrolyte, some of the original textile properties could be diminished accordingly. Therefore, it is not wise to neglect the development of the functional solid-state electrolyte, instead, more emphasis should be put on the detailed studies.

5.2.3 Proper Packaging Materials

As a matter of fact, it is rather difficult to find an universal material with all the desired properties. By contrast, works on studying the material with an individual function is more meaningful, such as the packaging materials. In most cases, the prepared the TWSCs cannot be directly used for the practical situation, due to the gel-electrolyte covered status. Thus, it is necessary to seek for the novel packaging materials and techniques for protecting the device.

Several strategies were presented to deal with the problem. As discussed before, PDMS has been widely used to encapsulate the assembled flexible SC, owing to the great transparency and excellent flexibility [124, 211]. In our previous work, the transparent silicone sealant was successfully adopted for sealing the 3D engraved SC, showing great flexibility and waterproofness [186]. Moreover, the PU and TPU functional films were also selected to package the device. In our previous work of 3D spacer fabric based SC, the functional PU film was successfully used for packaging

devices, displaying excellent device abrasion property and waterproofness [164]. Zheng's group also applied the TPU film to encapsulate the fabric based SC via a hot laminating method, and the device was well protected with excellent waterproof property [201].

5.3 Textile Technology Integration for Truly Compatible Products

Reviewing the reported works of the wearable SCs or other energy storage devices, focuses were substantially casted on the plain properties like flexibility and stretchability. Actually, as a wearable device, it is unreasonable to focus only on the chemical synthesis, staying away from textiles and the manufacturing technologies. Among the current studies, only a few works applied the strategy of developing the wearable SC from the perspective of textiles. In this regards, there is still large room in textile field to promote the further development of the TWSC and other devices.

5.3.1 Yarn Preparation Technology

Yarns are the fundamental units of textiles or garments, and their features can have large impact on the derived fabrics. It is almost the same case to fabricate a yarn electrode based SC device. Although tremendous works have been reported for developing the flexible SC with a fiber shape, very less of them underwent a real industrial processing for a final product [212-214]. As discussed in sec.3.1, yarns were fabricated through a series of processes, and for example, a cotton yarn usually undergoes the staple fiber integration, silver roving, spinning, twisting, winding, etc.. For a filament, techniques like melt spinning and wet spinning are widely used. Based on this, it is rational to start the preparation of the yarn electrode from each step of the procedures.

Decorating electroactive materials at the fiber stage. To gain a natural fiber based yarn, the first step is to integrate the staple fibers as the sliver, which lays the foundation for the following yarn fabrication. Thus, decorating the fibers at the very

beginning is beneficial to gain a highly loaded electrode. Also, the decorated fibers, with the light weight and small size, are capable of being processed to various textile electrodes, including yarn electrode and fabric electrode. Yury's group proposed the electrospinning of the biscalloped MXene and CNTs sheets for a fiber-shaped electrode, and the resulted device was successfully woven into a cotton fabric ^[127]. Zheng's group also decorated the CNT fiber by using the positive material MnO₂ and negative material Fe₃O₄. By applying the SHS (mentioned before), the nonwoven fabric electrodes made of the functional CNTs were successfully obtained, demonstrating an energy density even higher than that of the commercial organic SCs ^[201].

Applying the twisting technique. For the direct fabrication of the textile electrode, the strategy of twisting electroactive materials into a fiber has been widely reported, and some of the typical works were also discussed in the above sections. Apart from this, it is more practical to twist a fiber electrode with a common fiber for a composite fiber-shaped electrode that is tear resistant. In doing so, the electrode can be endowed with both electrochemical and mechanical properties, holding the promise that could be processed via the industrial-level machine. As the example shown in Fig.16.(b), a two-ply composite yarn electrode was obtained by twisting the AC-coated natural yarn with a stainless steel yarn. With the combined merits, the yarn electrode was successfully knitted as the fabric device ^[97]. On the contrary, twisting two different yarns is also advantageous for reduce the stiffness. As widely reported, the normal yarns, like cotton and nylon yarns, were twisted with the carbon fibers for accommodating the extra rigidity of the carbon fibers ^[215, 216].

Using the industrial coating technique. Dip-coating strategy was widely reported for enabling both the current collector layer and the electroactive material layer. Although it shows great merits in operating simplicity and convenience, it is not an accurate approach to gain the stable and convincing scientific results. However, the handle operation deserves an updating from the machine process level. As shown in Fig.22.(a), the industrial coating machine was originally adopted for realizing the

large-scale automated manufacturing of the electrode and the SC, resulting the MXene coated cotton and nylon yarns. After drying and winding, the yarns were directly knitted for a planar fabric SC via the flat-bed knitting machine ^[158].

5.3.2 Textile Technology Utilization

As the detailed introduction in Section 3 and 4, textiles and the manufacturing technologies showed intrinsic advantages in developing a wearable SC. Nevertheless, only limited of them were applied for SC, there is still much room for further studies. To provide an effective assistance to the future work, the relationship between textile technologies and their advantages is summarized in Table.2, where the correlation degree is classified from level I to level V, meaning the relevance from strong to weak, shown as below:

Table.2 Textile technologies and the advantages.

Textile Technology	Load Mass	Stretchability	Washability	Breathability	Compatibility
Core-shell Yarn	III-IV	II-III	IV-V	I - II	I - II
Integrated Yarn	II-III	III-IV	II-III	I - II	I - II
Functionalizing Knit Fabric	III-IV	III-IV	IV-V	III-IV	III-IV
Knit SC	II-III	II-III	II-III	I - II	II-III
Functionalizing Woven Fabric	IV	IV-V	IV-V	IV-V	III-IV
Woven SC	III-IV	IV-V	II-III	IV-V	II-III
Functionalized Nonwoven Fabric	IV-V	IV-V	IV-V	V	IV-V
Nonwoven Technique	II-III	IV-V	II-III	IV-V	IV-V
Printing	II-III	III-IV	IV-V	IV-V	II-III
Sewing	II-III	III-V	III-V	II-III	I - II
Embroidering	III-IV	III-V	III-V	II-III	I - II

3D Knitting	III-IV	III-V	III-V	III-V	II-III
-------------	--------	-------	-------	-------	--------

6 Summary and Outlook

Flexible and wearable supercapacitors are currently held with great promise to provide the energy sources for the smart and wearable applications. The past decade has witnessed the booming of the significant progress made in both fundamental studies and the device developments, yet still remaining challenges in the practical applications. This review is dedicated to covering the recent progress in textile substrate and wearable technologies derived supercapacitors, with a focus on the main advantages and improving strategies.

It has started up with detailing the fundamental mechanisms of SC and manufacturing technologies of textiles. The EDLC and PDC based energy storing mechanisms are introduced and analyzed with batteries, and the unique feature of SCs in better power density is also highlighted. The fundamental textiles and typical manufacturing technologies are then presented in details, including the information of yarn type and fabrication, knitting fabric, woven fabric, nonwoven fabric, printed fabric, sewn fabric, embroidery, and the 3D spacing fabric. Based on the unique features of textile substrates and technologies, the typical and recent developed TWSCs are reviewed in terms of the advantages in flexibility, stretchability, washability, breathability and compatibility.

To promote the future development of TWSC, the strategies for improving the overall performances are proposed from the perspective of the textiles. First and foremost, as an applied device, it is the basic requirement for TWSCs to be bearing with sufficient electrochemical performance to meet the practical demand. The electroactive material loading issue is the critical factor, and thus, strategies for increasing the mass on the textile substrates or via the textile manufacturing technologies are presented properly. For the functionalized textile electrode, it is advised to apply the strategies of using

conductive electroactive materials, engineering porous nanostructures, porous nanostructures, adopting novel electrode preparation method, and suppressing material delamination. As for the textile electrode, it lies in using conductive electroactive materials, fabricating electrode without additives and seeking for more textile techniques.

To further consolidate the multifunctions of TWSCs, strategies from the viewpoint of materials are proposed correspondingly, including the stretchable, washable, and wear-resistant electroactive materials, stretchable and robust solid-state electrolyte, and proper packaging materials. Considering the practical application of TWSCs, strategies in view of textile and technologies are advised. For yarn electrode fabrication, it is expected to pose emphasis on aspects of decorating electroactive materials at the fiber scale, applying the twisting technique, and using the industrial coating technique. To fabricate a proper textile electrode, more textile technologies are needed to be introduced. For the convenience of the future work in using textile based strategies, we summarized the relationship between textile technologies and their advantages in the table, labeling the correlation degree with different level numbers.

Using existing electrode materials and flexible substrate as a starting point, the development of TWSC exhibits promising future for satisfying the energy demand from the smart textiles and electronics, yet to be realized. There are various pathways to design novel materials and device structures from the viewpoint of textiles and their manufacturing technologies, which can help to reach the desired electrochemical performance and the wearable demand in the everyday-use level. Supercapacitors derived from the textile perspective offer glimpses of the functional and truly flexible high power devices.

Glossary:

3DAS:	three dimensional spacer fabric based asymmetric supercapacitor(s)
3DSF:	three dimensional spacer fabric
ACFT:	activated carbon fiber textile
ACN:	acetonitrile
AC-St-NFW:	AC-coated yarn with a stainless steel yarn
ATC:	activated textile carbon
AuNF:	Au coated nanofiber
BMX:	biscrolling MXene
CC:	carbon cloth
CH:	carbonate hydroxide
CNOs:	carbon nano-onions
CF:	carbon fiber
CFT:	carbon fiber thread
CNF(s):	carbon nanofiber(s)
CNT:	carbon nanotube
CNTFFs:	CNT fiber fabrics
CS(s):	carbon spheres
CV:	cyclic voltammetry
EACF:	electrochemically activated carbon fiber
EDLC(s):	electrical double-layer capacitors
EIS:	electrochemical impedance spectroscopy
E-textile(s):	electronic textile(s)
GCD:	galvanostatic charge and discharge
GO:	graphene oxide
GN(s):	graphene nanosheet(s)
GNP:	graphene nanoplate
PAN:	polyacrylonitrile
PC:	propylene carbonate
PEDOT:PSS:	poly(3,4-ethylenedioxythiophene): poly(styrenesulfonate)

PMMA:	poly(methyl methacrylate)
PPy:	polypyrrole
PPyG:	PPy granula
PU:	polyurethane
PVA:	polyvinyl alcohol
rGO:	reduced graphene oxide
SC(s):	supercapacitor(s)
SCE:	saturated calomel electrode
SPNF(s):	silver-plated nylon fiber(s)
SPNY(s):	silver-plated nylon yarn(s)
SSY:	stainless steel yarn
TSC(s):	textile-based supercapacitors
VPPyNTs:	vertical PPy nanotubes

Acknowledgment:

The authors acknowledge The Hong Kong Polytechnic University for funding supports (Project No. G-YWA2 and G-YZ4H) of this work.

References

- [1] Alargova, R.G., K.H. Bhatt, V.N. Paunov, and O.D. Velev, Scalable Synthesis of a New Class of Polymer Microrods by a Liquid-Liquid Dispersion Technique. *Advanced Materials* 2004. **16**(18), 1653-1657.
- [2] Guo, Y., X. Tao, B. Xu, J. Feng, and S. Wang, Structural characteristics of low torque and ring spun yarns. *Textile research journal* 2011. **81**(8), 778-790.
- [3] Li, J. and B. Xu, Novel highly sensitive and wearable pressure sensors from conductive three-dimensional fabric structures. *Smart Materials and Structures* 2015. **24**(12),
- [4] Chen, Y., B. Xu, J. Xu, J. Wen, T. Hua, and C.-W. Kan, Graphene-based in-planar supercapacitors by a novel laser-scribing, in-situ reduction and transfer-printed method on flexible substrates. *Journal of Power Sources* 2019. **420**, 82-87.
- [5] Liu, F. and D. Xue, Advanced graphene nanomaterials for electrochemical energy storage. *Materials Research Innovations* 2014. **19**(1), 7-19.
- [6] Lu, X., T. Zhai, X. Zhang, Y. Shen, L. Yuan, B. Hu, L. Gong, J. Chen, Y. Gao, J. Zhou, Y. Tong, and Z.L. Wang, WO₃-x@Au@MnO₂ Core-Shell Nanowires on Carbon Fabric for

- High-Performance Flexible Supercapacitors. *Advanced Materials* 2012. **24**(7), 938-944.
- [7] Liu, N., W. Ma, J. Tao, X. Zhang, J. Su, L. Li, C. Yang, Y. Gao, D. Golberg, and Y. Bando, Cable - Type Supercapacitors of Three - Dimensional Cotton Thread Based Multi - Grade Nanostructures for Wearable Energy Storage. *Advanced Materials* 2013. **25**(35), 4925-4931.
- [8] Ren, J., L. Li, C. Chen, X. Chen, Z. Cai, L. Qiu, Y. Wang, X. Zhu, and H. Peng, Twisting Carbon Nanotube Fibers for Both Wire - Shaped Micro - Supercapacitor and Micro - Battery. *Advanced Materials* 2013. **25**(8), 1155-1159.
- [9] Miller, J.R., Valuing reversible energy storage. *Science* 2012. **335**(6074), 1312-1313.
- [10] Lu, X., M. Yu, G. Wang, Y. Tong, and Y. Li, Flexible solid-state supercapacitors: design, fabrication and applications. *Energy & Environmental Science* 2014. **7**(7), 2160.
- [11] Jost, K., C.R. Perez, J.K. McDonough, V. Presser, M. Heon, G. Dion, and Y. Gogotsi, Carbon coated textiles for flexible energy storage. *Energy & Environmental Science* 2011. **4**(12), 5060-5067.
- [12] Cai, G., P. Darmawan, M. Cui, J. Wang, J. Chen, S. Magdassi, and P.S. Lee, Supercapacitors: Highly Stable Transparent Conductive Silver Grid/PEDOT: PSS Electrodes for Integrated Bifunctional Flexible Electrochromic Supercapacitors (*Adv. Energy Mater.* 4/2016). *Advanced Energy Materials* 2016. **6**(4),
- [13] Chee, W.K., H.N. Lim, Z. Zainal, N.M. Huang, I. Harrison, and Y. Andou, Flexible Graphene-Based Supercapacitors: A Review. *The Journal of Physical Chemistry C* 2016. **120**(8), 4153-4172.
- [14] Dogru, I.B., M.B. Durukan, O. Turel, and H.E. Unalan, Flexible supercapacitor electrodes with vertically aligned carbon nanotubes grown on aluminum foils. *Progress in Natural Science: Materials International* 2016. **26**(3), 232-236.
- [15] Wang, X., X. Lu, B. Liu, D. Chen, Y. Tong, and G. Shen, Flexible Energy - Storage Devices: Design Consideration and Recent Progress. *Advanced Materials* 2014. **26**(28), 4763-4782.
- [16] Lee, S.-Y., K.-H. Choi, W.-S. Choi, Y.H. Kwon, H.-R. Jung, H.-C. Shin, and J.Y. Kim, Progress in flexible energy storage and conversion systems, with a focus on cable-type lithium-ion batteries. *Energy & Environmental Science* 2013. **6**(8), 2414-2423.
- [17] Chan, M., D. Esteve, J.Y. Fourniols, C. Escriba, and E. Campo, Smart wearable systems: current status and future challenges. *Artif Intell Med* 2012. **56**(3), 137-56.
- [18] Dong, L., C. Xu, Y. Li, Z.-H. Huang, F. Kang, Q.-H. Yang, and X. Zhao, Flexible electrodes and supercapacitors for wearable energy storage: a review by category. *J. Mater. Chem. A* 2016. **4**(13), 4659-4685.
- [19] Ghahremani Honarvar, M. and M. Latifi, Overview of wearable electronics and smart textiles. *The Journal of The Textile Institute* 2016. **108**(4), 631-652.
- [20] Pu, X., L. Li, M. Liu, C. Jiang, C. Du, Z. Zhao, W. Hu, and Z.L. Wang, Wearable Self-Charging Power Textile Based on Flexible Yarn Supercapacitors and Fabric Nanogenerators. *Adv Mater* 2016. **28**(1), 98-105.
- [21] Wang, X., B. Liu, R. Liu, Q. Wang, X. Hou, D. Chen, R. Wang, and G. Shen, Fiber-based flexible all-solid-state asymmetric supercapacitors for integrated photodetecting system. *Angew Chem Int Ed Engl* 2014. **53**(7), 1849-53.
- [22] Torop, J., V. Palmre, M. Arulepp, T. Sugino, K. Asaka, and A. Aabloo, Flexible supercapacitor-like actuator with carbide-derived carbon electrodes. *Carbon* 2011. **49**(9), 3113-3119.
- [23] Vangari, M., T. Pryor, and L. Jiang, Supercapacitors: review of materials and fabrication methods.

- Journal of Energy Engineering 2012. **139**(2), 72-79.
- [24] Yuan, L., X. Xiao, T. Ding, J. Zhong, X. Zhang, Y. Shen, B. Hu, Y. Huang, J. Zhou, and Z.L. Wang, Paper-based supercapacitors for self-powered nanosystems. *Angew Chem Int Ed Engl* 2012. **51**(20), 4934-8.
 - [25] Fan, X., W. Nie, H. Tsai, N. Wang, H. Huang, Y. Cheng, R. Wen, L. Ma, F. Yan, and Y. Xia, PEDOT:PSS for Flexible and Stretchable Electronics: Modifications, Strategies, and Applications. *Adv Sci (Weinh)* 2019. **6**(19), 1900813.
 - [26] Augustyn, V., P. Simon, and B. Dunn, Pseudocapacitive oxide materials for high-rate electrochemical energy storage. *Energy & Environmental Science* 2014. **7**(5),
 - [27] Lin, Z., E. Goikolea, A. Balducci, K. Naoi, P.L. Taberna, M. Salanne, G. Yushin, and P. Simon, Materials for supercapacitors: When Li-ion battery power is not enough. *Materials Today* 2018. **21**(4), 419-436.
 - [28] Abruña, H.D., Y. Kiya, and J.C. Henderson, Batteries and electrochemical capacitors. *Physics Today* 2008.
 - [29] Shao, H., Y.-C. Wu, Z. Lin, P.-L. Taberna, and P. Simon, Nanoporous carbon for electrochemical capacitive energy storage. *Chemical Society Reviews* 2020. **49**(10), 3005-3039.
 - [30] Simon, P. and Y. Gogotsi, Materials for electrochemical capacitors, in *Nanoscience And Technology: A Collection of Reviews from Nature Journals*. 2010, World Scientific. p. 320-329.
 - [31] Conway, B.E., Electrochemical supercapacitors: scientific fundamentals and technological applications. 2013: Springer Science & Business Media.
 - [32] Gogotsi, Y. and P. Simon, True performance metrics in electrochemical energy storage. *Science* 2011. **334**(6058), 917-918.
 - [33] Choi, C., D.S. Ashby, D.M. Butts, R.H. DeBlock, Q. Wei, J. Lau, and B. Dunn, Achieving high energy density and high power density with pseudocapacitive materials. *Nature Reviews Materials* 2020. **5**(1), 5-19.
 - [34] González, A., E. Goikolea, J.A. Barrena, and R. Mysyk, Review on supercapacitors: Technologies and materials. *Renewable and Sustainable Energy Reviews* 2016. **58**, 1189-1206.
 - [35] Shi, F., L. Li, X.-l. Wang, C.-d. Gu, and J.-p. Tu, Metal oxide/hydroxide-based materials for supercapacitors. *Rsc Advances* 2014. **4**(79), 41910-41921.
 - [36] Brousse, T., D. Bélanger, and J.W. Long, To Be or Not To Be Pseudocapacitive? *Journal of The Electrochemical Society* 2015. **162**(5), A5185-A5189.
 - [37] Hung, D.Q., M.R. Shah, and N. Mithulananthan, Technical Challenges, Security and Risk in Grid Integration of Renewable Energy, in *Smart Power Systems and Renewable Energy System Integration*. 2016, Springer. p. 99-118.
 - [38] Fisher, R.A., M.R. Watt, R. Konjeti, and W.J. Ready, Atomic Layer Deposition of Titanium Oxide for Pseudocapacitive Functionalization of Vertically-Aligned Carbon Nanotube Supercapacitor Electrodes. *ECS Journal of Solid State Science and Technology* 2015. **4**(2), M1-M5.
 - [39] Simon, P. and Y. Gogotsi, Perspectives for electrochemical capacitors and related devices. *Nature Materials* 2020. **19**(11), 1151-1163.
 - [40] Simon, P. and Y. Gogotsi, Charge storage mechanism in nanoporous carbons and its consequence for electrical double layer capacitors. *Philosophical Transactions of the Royal Society A: Mathematical, Physical and Engineering Sciences* 2010. **368**(1923), 3457-3467.

- [41] Tomaszewska, A., Z. Chu, X. Feng, S. O'Kane, X. Liu, J. Chen, C. Ji, E. Endler, R. Li, L. Liu, Y. Li, S. Zheng, S. Vetterlein, M. Gao, J. Du, M. Parkes, M. Ouyang, M. Marinescu, G. Offer, and B. Wu, Lithium-ion battery fast charging: A review. *eTransportation* 2019. **1**,
- [42] Taberna, P.L., S. Mitra, P. Poizot, P. Simon, and J.M. Tarascon, High rate capabilities Fe₃O₄-based Cu nano-architected electrodes for lithium-ion battery applications. *Nature Materials* 2006. **5**(7), 567-573.
- [43] Li, L., Z. Wu, S. Yuan, and X.-B. Zhang, Advances and challenges for flexible energy storage and conversion devices and systems. *Energy & Environmental Science* 2014. **7**(7), 2101-2122.
- [44] Salanne, M., B. Rotenberg, K. Naoi, K. Kaneko, P.L. Taberna, C.P. Grey, B. Dunn, and P. Simon, Efficient storage mechanisms for building better supercapacitors. *Nature Energy* 2016. **1**(6),
- [45] Miller, J.R. and P. Simon, Fundamentals of electrochemical capacitor design and operation. *Electrochem. Soc. Interface* 2008. **17**(1), 31-2.
- [46] Zhao, W., L. Wei, Q. Fu, and X. Guo, High-performance, flexible, solid-state micro-supercapacitors based on printed asymmetric interdigital electrodes and bio-hydrogel for on-chip electronics. *Journal of Power Sources* 2019. **422**, 73-83.
- [47] Wen, J., B. Xu, J. Zhou, and Y. Chen, Novel high-performance asymmetric supercapacitors based on nickel-cobalt composite and PPy for flexible and wearable energy storage. *Journal of Power Sources* 2018. **402**, 91-98.
- [48] Ashir, M., C. Sennewald, G. Hoffmann, and C. Cherif, Development of Woven Spacer Fabrics Based on Steel Wires and Carbon Rovings. *Fibres and Textiles in Eastern Europe* 2017. **25**(0), 49-55.
- [49] Wang, Z., J. Cheng, Q. Guan, H. Huang, Y. Li, J. Zhou, W. Ni, B. Wang, S. He, and H. Peng, All-in-one fiber for stretchable fiber-shaped tandem supercapacitors. *Nano Energy* 2018. **45**, 210-219.
- [50] Dong, K., Y.C. Wang, J. Deng, Y. Dai, S.L. Zhang, H. Zou, B. Gu, B. Sun, and Z.L. Wang, A Highly Stretchable and Washable All-Yarn-Based Self-Charging Knitting Power Textile Composed of Fiber Triboelectric Nanogenerators and Supercapacitors. *ACS Nano* 2017. **11**(9), 9490-9499.
- [51] Wen, J., B. Xu, and J. Zhou, Toward Flexible and Wearable Embroidered Supercapacitors from Cobalt Phosphides-Decorated Conductive Fibers. *Nano-Micro Letters* 2019. **11**(1),
- [52] Lei, S., Y. Liu, L. Fei, R. Song, W. Lu, L. Shu, C.L. Mak, Y. Wang, and H. Huang, Commercial Dacron cloth supported Cu(OH)₂ nanobelt arrays for wearable supercapacitors. *Journal of Materials Chemistry A* 2016. **4**(38), 14781-14788.
- [53] Li, Z., M. Tian, X. Sun, H. Zhao, S. Zhu, and X. Zhang, Flexible all-solid planar fibrous cellulose nonwoven fabric-based supercapacitor via capillarity-assisted graphene/MnO₂ assembly. *Journal of Alloys and Compounds* 2019. **782**, 986-994.
- [54] Zhang, C.J., L. McKeon, M.P. Kremer, S.H. Park, O. Ronan, A. Seral-Ascaso, S. Barwich, C.O. Coileain, N. McEvoy, H.C. Nerl, B. Anasori, J.N. Coleman, Y. Gogotsi, and V. Nicolosi, Additive-free MXene inks and direct printing of micro-supercapacitors. *Nat Commun* 2019. **10**(1), 1795.
- [55] Yang, Y., Q. Huang, L. Niu, D. Wang, C. Yan, Y. She, and Z. Zheng, Waterproof, Ultrahigh Areal-Capacitance, Wearable Supercapacitor Fabrics. *Adv Mater* 2017.
- [56] Balasingam, S.K., A. Thirumurugan, J.S. Lee, and Y. Jun, Amorphous MoS_x thin-film-coated carbon fiber paper as a 3D electrode for long cycle life symmetric supercapacitors. *Nanoscale*

2016. **8**(23), 11787-91.

- [57] Chodankar, N.R., H.D. Pham, A.K. Nanjundan, J.F.S. Fernando, K. Jayaramulu, D. Golberg, Y.K. Han, and D.P. Dubal, True Meaning of Pseudocapacitors and Their Performance Metrics: Asymmetric versus Hybrid Supercapacitors. *Small* 2020. e2002806.
- [58] Farid, M.M., A.M. Khudhair, S.A.K. Razack, and S. Al-Hallaj, A review on phase change energy storage: materials and applications. *Energy conversion and management* 2004. **45**(9), 1597-1615.
- [59] Lin, L., W. Lei, S. Zhang, Y. Liu, G.G. Wallace, and J. Chen, Two-dimensional transition metal dichalcogenides in supercapacitors and secondary batteries. *Energy Storage Materials* 2019. **19**, 408-423.
- [60] Liu, L., Z. Niu, and J. Chen, Flexible supercapacitors based on carbon nanotubes. *Chinese Chemical Letters* 2018. **29**(4), 571-581.
- [61] Bose, S., T. Kuila, A.K. Mishra, R. Rajasekar, N.H. Kim, and J.H. Lee, Carbon-based nanostructured materials and their composites as supercapacitor electrodes. *Journal of Materials Chemistry* 2012. **22**(3), 767-784.
- [62] Tung, V.C., M.J. Allen, Y. Yang, and R.B. Kaner, High-throughput solution processing of large-scale graphene. *Nature nanotechnology* 2008. **4**(1), nano. 2008.329.
- [63] Zaanen, J., G. Sawatzky, and J. Allen, Band gaps and electronic structure of transition-metal compounds. *Physical Review Letters* 1985. **55**(4), 418.
- [64] Hsieh, T.-F., C.-C. Chuang, W.-J. Chen, J.-H. Huang, W.-T. Chen, and C.-M. Shu, Hydrous ruthenium dioxide/multi-walled carbon-nanotube/titanium electrodes for supercapacitors. *Carbon* 2012. **50**(5), 1740-1747.
- [65] Chen, W., X. Pan, M.-G. Willinger, D.S. Su, and X. Bao, Facile autoreduction of iron oxide/carbon nanotube encapsulates. *Journal of the American Chemical Society* 2006. **128**(10), 3136-3137.
- [66] Amade, R., E. Jover, B. Caglar, T. Mutlu, and E. Bertran, Optimization of MnO₂/vertically aligned carbon nanotube composite for supercapacitor application. *Journal of Power Sources* 2011. **196**(13), 5779-5783.
- [67] Bao, F., Z. Zhang, W. Guo, and X. Liu, Facile Synthesis of Three Dimensional NiCo₂O₄@MnO₂ Core-Shell Nanosheet Arrays and its Supercapacitive Performance. *Electrochimica Acta* 2015. **157**, 31-40.
- [68] Chen, S., L. Wang, M. Huang, L. Kang, Z. Lei, H. Xu, F. Shi, and Z.-H. Liu, Reduced graphene oxide/Mn₃O₄ nanocrystals hybrid fiber for flexible all-solid-state supercapacitor with excellent volumetric energy density. *Electrochimica Acta* 2017. **242**, 10-18.
- [69] Wang, X., X. Han, M. Lim, N. Singh, C.L. Gan, M. Jan, and P.S. Lee, Nickel Cobalt Oxide-Single Wall Carbon Nanotube Composite Material for Superior Cycling Stability and High-Performance Supercapacitor Application. *The Journal of Physical Chemistry C* 2012. **116**(23), 12448-12454.
- [70] Wei, T.Y., C.H. Chen, H.C. Chien, S.Y. Lu, and C.C. Hu, A cost-effective supercapacitor material of ultrahigh specific capacitances: spinel nickel cobaltite aerogels from an epoxide-driven sol-gel process. *Adv Mater* 2010. **22**(3), 347-51.
- [71] Chien, H.C., W.Y. Cheng, Y.H. Wang, and S.Y. Lu, Ultrahigh specific capacitances for supercapacitors achieved by nickel cobaltite/carbon aerogel composites. *Advanced Functional Materials* 2012. **22**(23), 5038-5043.
- [72] Jiang, H., J. Ma, and C. Li, Hierarchical porous NiCo₂O₄ nanowires for high-rate

- supercapacitors. *Chemical communications* 2012. **48**(37), 4465-4467.
- [73] Zhu, S., L. Li, J. Liu, H. Wang, T. Wang, Y. Zhang, L. Zhang, R.S. Ruoff, and F. Dong, Structural Directed Growth of Ultrathin Parallel Birnessite on β -MnO₂ for High-Performance Asymmetric Supercapacitors. *ACS Nano* 2018. **12**(2), 1033-1042.
- [74] Balogun, M.S., W. Qiu, J. Jian, Y. Huang, Y. Luo, H. Yang, C. Liang, X. Lu, and Y. Tong, Vanadium Nitride Nanowire Supported SnS₂ Nanosheets with High Reversible Capacity as Anode Material for Lithium Ion Batteries. *ACS Appl Mater Interfaces* 2015. **7**(41), 23205-15.
- [75] Choi, D., G.E. Blomgren, and P.N. Kumta, Fast and reversible surface redox reaction in nanocrystalline vanadium nitride supercapacitors. *Advanced Materials* 2006. **18**(9), 1178-1182.
- [76] Zhao, J., C. Li, Q. Zhang, J. Zhang, X. Wang, J. Sun, J. Wang, J. Xie, C. Lu, W. Lu, and Y. Yao, All-solid-state hybrid supercapacitors based on ZnCo₂O₄ nanowire arrays and carbon nanorod electrode materials. *Carbon* 2017. **123**, 676-682.
- [77] Li, J., X. Yuan, C. Lin, Y. Yang, L. Xu, X. Du, J. Xie, J. Lin, and J. Sun, Achieving High Pseudocapacitance of 2D Titanium Carbide (MXene) by Cation Intercalation and Surface Modification. *Advanced Energy Materials* 2017. **7**(15),
- [78] Mohammad Shiri, H., A. Ehsani, and M. Jalali Khales, Electrochemical synthesis of Sm₂O₃ nanoparticles: Application in conductive polymer composite films for supercapacitors. *J Colloid Interface Sci* 2017. **505**, 940-946.
- [79] Yuksel, R., A. Ekber, J. Turan, E. Alpugan, S.O. Hacioglu, L. Toppare, A. Cirpan, G. Gunbas, and H.E. Unalan, A Novel Blue to Transparent Polymer for Electrochromic Supercapacitor Electrodes. *Electroanalysis* 2018. **30**(2), 266-273.
- [80] Bober, P., N. Gavrilov, A. Kovalcik, M. Mičušik, C. Unterweger, I.A. Pašti, I. Šeděnková, U. Acharya, J. Pflieger, S.K. Filippov, J. Kuliček, M. Omastová, S. Breitenbach, G. Čirić-Marjanović, and J. Stejskal, Electrochemical properties of lignin/polypyrrole composites and their carbonized analogues. *Materials Chemistry and Physics* 2018. **213**, 352-361.
- [81] Wan, P., X. Wen, C. Sun, B.K. Chandran, H. Zhang, X. Sun, and X. Chen, Flexible Transparent Films Based on Nanocomposite Networks of Polyaniline and Carbon Nanotubes for High - Performance Gas Sensing. *Small* 2015. **11**(40), 5409-5415.
- [82] Snook, G.A., P. Kao, and A.S. Best, Conducting-polymer-based supercapacitor devices and electrodes. *Journal of Power Sources* 2011. **196**(1), 1-12.
- [83] Peng, T., W. Sun, C. Huang, W. Yu, B. Sebo, Z. Dai, S. Guo, and X.-Z. Zhao, Self-assembled free-standing polypyrrole nanotube membrane as an efficient FTO-and Pt-free counter electrode for dye-sensitized solar cells. *ACS applied materials & interfaces* 2013. **6**(1), 14-17.
- [84] Fisher, R.A., M.R. Watt, and W.J. Ready, Functionalized carbon nanotube supercapacitor electrodes: a review on pseudocapacitive materials. *ECS Journal of Solid State Science and Technology* 2013. **2**(10), M3170-M3177.
- [85] Lokhande, V.C., A.C. Lokhande, C.D. Lokhande, J.H. Kim, and T. Ji, Supercapacitive composite metal oxide electrodes formed with carbon, metal oxides and conducting polymers. *Journal of Alloys and Compounds* 2016. **682**, 381-403.
- [86] Genovese, M., Y.W. Foong, and K. Lian, The unique properties of aqueous polyoxometalate (POM) mixtures and their role in the design of molecular coatings for electrochemical energy storage. *Electrochimica Acta* 2016. **199**, 261-269.
- [87] Genovese, M. and K. Lian, Polyoxometalate modified pine cone biochar carbon for supercapacitor

- electrodes. *Journal of Materials Chemistry A* 2017. **5**(8), 3939-3947.
- [88] Yu, F., T. Wang, Z. Wen, and H. Wang, High performance all-solid-state symmetric supercapacitor based on porous carbon made from a metal-organic framework compound. *Journal of Power Sources* 2017. **364**, 9-15.
- [89] Halder, A., M. Ghosh, M.A. Khayum, S. Bera, M. Addicoat, H.S. Sasmal, S. Karak, S. Kurungot, and R. Banerjee, Interlayer Hydrogen-Bonded Covalent Organic Frameworks as High-Performance Supercapacitors. *J Am Chem Soc* 2018. **140**(35), 10941-10945.
- [90] Wang, Q., Y. Luo, R. Hou, S. Zaman, K. Qi, H. Liu, H.S. Park, and B.Y. Xia, Redox Tuning in Crystalline and Electronic Structure of Bimetal-Organic Frameworks Derived Cobalt/Nickel Boride/Sulfide for Boosted Faradaic Capacitance. *Adv Mater* 2019. **31**(51), e1905744.
- [91] Köpf, M., N. Eckstein, D. Pfister, C. Grotz, I. Krüger, M. Greiwe, T. Hansen, H. Kohlmann, and T. Nilges, Access and in situ growth of phosphorene-precursor black phosphorus. *Journal of crystal growth* 2014. **405**, 6-10.
- [92] Hao, C., B. Yang, F. Wen, J. Xiang, L. Li, W. Wang, Z. Zeng, B. Xu, Z. Zhao, Z. Liu, and Y. Tian, Flexible All-Solid-State Supercapacitors based on Liquid-Exfoliated Black-Phosphorus Nanoflakes. *Adv Mater* 2016. **28**(16), 3194-201.
- [93] Wen, M., D. Liu, Y. Kang, J. Wang, H. Huang, J. Li, P.K. Chu, and X.-F. Yu, Synthesis of high-quality black phosphorus sponges for all-solid-state supercapacitors. *Materials Horizons* 2019. **6**(1), 176-181.
- [94] Nie, G., X. Lu, J. Lei, L. Yang, and C. Wang, Facile and controlled synthesis of bismuth sulfide nanorods-reduced graphene oxide composites with enhanced supercapacitor performance. *Electrochimica Acta* 2015. **154**, 24-30.
- [95] Pan, U.N., V. Sharma, T. Kshetri, T.I. Singh, D.R. Paudel, N.H. Kim, and J.H. Lee, Freestanding 1T-Mnx Mo1- x S2- y Sey and MoFe2 S4- z Sez Ultrathin Nanosheet-Structured Electrodes for Highly Efficient Flexible Solid-State Asymmetric Supercapacitors. *Small* 2020. e2001691.
- [96] Liu, H., X. Tao, K. Choi, and B. Xu, Analysis of the relaxation modulus of spun yarns. *Textile research journal* 2010. **80**(5), 403-410.
- [97] Jost, K., D.P. Durkin, L.M. Haverhals, E.K. Brown, M. Langenstein, H.C. De Long, P.C. Trulove, Y. Gogotsi, and G. Dion, Natural Fiber Welded Electrode Yarns for Knittable Textile Supercapacitors. *Advanced Energy Materials* 2015. **5**(4), 1401286.
- [98] Gong, J., B. Xu, X. Guan, Y. Chen, S. Li, and J. Feng, Towards truly wearable energy harvesters with full structural integrity of fiber materials. *Nano Energy* 2019. **58**, 365-374.
- [99] Zhang, X., Y. Zheng, W. Zheng, W. Zhao, and D. Chen, Graphite felt decorated with porous NiCo 2 O 4 nanosheets for high-performance pseudocapacitor electrodes. *Journal of Materials Science* 2017. **52**(9), 5179-5187.
- [100] Liang, Z., B. Xu, Z. Chi, and D. Feng, Intelligent characterization and evaluation of yarn surface appearance using saliency map analysis, wavelet transform and fuzzy ARTMAP neural network. *Expert Systems with Applications* 2012. **39**(4), 4201-4212.
- [101] Lee, J.A., A.E. Aliev, J.S. Bykova, M.J. de Andrade, D. Kim, H.J. Sim, X. Lepro, A.A. Zakhidov, J.B. Lee, G.M. Spinks, S. Roth, S.J. Kim, and R.H. Baughman, Woven-Yarn Thermoelectric Textiles. *Adv Mater* 2016. **28**(25), 5038-44.
- [102] Ishmael, N., A. Fernando, S. Andrew, and L. Waterton Taylor, Textile technologies for the manufacture of three-dimensional textile preforms. *Research Journal of Textile and Apparel* 2017. **21**(4), 342-362.

- [103] Pourmohammadi, A., Nonwoven materials and joining techniques, in *Joining Textiles*. 2013. p. 565-581.
- [104] Wang, K.Y., L.M. Demeny, W.S. Pomplun, P.S. Mumick, R.L. Anderson, and J.F. Merker, Dispersible nonwoven fabric and method of making same. 1999, Google Patents.
- [105] Briggs-Goode, A. and A. Russell, Printed textile design, in *Textile Design*. 2011, Elsevier. p. 105-129e.
- [106] Chequer, F.D., G.A.R. de Oliveira, E.A. Ferraz, J.C. Cardoso, M.B. Zanoni, and D.P. de Oliveira, Textile dyes: dyeing process and environmental impact. *Eco-friendly textile dyeing and finishing* 2013. **6**, 151-176.
- [107] Hakamada, S., S. Koike, and K. Shirota, Printing process, print obtained by the process and processed article. 2004, Google Patents.
- [108] Sonoda, H., Sewing conformal field theories II. *Nuclear Physics B* 1988. **311**(2), 417-432.
- [109] Choudhary, A.K., M.P. Sikka, and P. Bansal, The study of sewing damage and defects in garments. *Research Journal of Textile and Apparel* 2018.
- [110] Ahmed, J. and W. Al-Khyatt, LRYGB: The hand-sewn technique, in *Obesity, Bariatric and Metabolic Surgery*. 2016, Springer. p. 191-196.
- [111] Hamdan, N.A.-h., S. Voelker, and J. Borchers, Sketch&Stitch, in *Proceedings of the 2018 CHI Conference on Human Factors in Computing Systems - CHI '18*. 2018. p. 1-13.
- [112] Gil, I., R. Fernández-García, and J.A. Tornero, Embroidery manufacturing techniques for textile dipole antenna applied to wireless body area network. *Textile Research Journal* 2018. **89**(8), 1573-1581.
- [113] Li, J. and B. Xu, Novel highly sensitive and wearable pressure sensors from conductive three-dimensional fabric structures. *Smart Materials and Structures* 2015. **24**(12), 125022.
- [114] Dow, M.B. and H.B. Dexter, Development of stitched, braided and woven composite structures in the ACT program and at Langley Research Center. 1997.
- [115] Bader, M.G., Microstructural design of fiber composites. By Tsu - Wei Chou, Cambridge University Press, Cambridge 1992, X, 569 pp, hardback, \$150, ISBN 0 - 523 - 35482. *Advanced Materials* 1992. **4**(10), 693-694.
- [116] Peterson, J., E. Vegborn, and C.-H. Andersson, Knittability of fibres with high stiffness. in *Conference on Mechanics of Composite Materials 2000*, Riga, Lettland. 2000.
- [117] Li, X., G. Jiang, X. Nie, P. Ma, and Z. Gao, Knitting Technologies And Tensile Properties Of A Novel Curved Flat-Knitted Three-Dimensional Spacer Fabrics. *Autex Research Journal* 2015. **15**(3), 191-197.
- [118] Knittel, C., D. Nicholas, R. Street, C. Schauer, and G. Dion, Self-Folding Textiles through Manipulation of Knit Stitch Architecture. *Fibers* 2015. **3**(4), 575-587.
- [119] Han, F., H. Chen, K. Jiang, W. Zhang, T. Lv, and Y. Yang, Influences of geometric patterns of 3D spacer fabric on tensile behavior of concrete canvas. *Construction and Building Materials* 2014. **65**, 620-629.
- [120] Soin, N., T.H. Shah, S.C. Anand, J. Geng, W. Pornwannachai, P. Mandal, D. Reid, S. Sharma, R.L. Hadimani, D.V. Bayramol, and E. Siores, Novel "3-D spacer" all fibre piezoelectric textiles for energy harvesting applications. *Energy Environ. Sci.* 2014. **7**(5), 1670-1679.
- [121] Zhang, X., Q. Fu, H. Huang, L. Wei, and X. Guo, Silver-Quantum-Dot-Modified MoO₃ and MnO₂ Paper-Like Freestanding Films for Flexible Solid-State Asymmetric Supercapacitors. *Small* 2019. **15**(13), e1805235.

- [122] Wang, C., X. Wu, Y. Ma, G. Mu, Y. Li, C. Luo, H. Xu, Y. Zhang, J. Yang, and X. Tang, Metallic few-layered VSe₂ nanosheets: high two-dimensional conductivity for flexible in-plane solid-state supercapacitors. *Journal of Materials Chemistry A* 2018. **6**(18), 8299-8306.
- [123] Chen, D., K. Jiang, T. Huang, and G. Shen, Recent Advances in Fiber Supercapacitors: Materials, Device Configurations, and Applications. *Adv Mater* 2019. e1901806.
- [124] Chen, Y., B. Xu, J. Wen, J. Gong, T. Hua, C.W. Kan, and J. Deng, Design of Novel Wearable, Stretchable, and Waterproof Cable-Type Supercapacitors Based on High-Performance Nickel Cobalt Sulfide-Coated Etching-Annealed Yarn Electrodes. *Small* 2018. **14**(21), e1704373.
- [125] Ai, Y., Z. Lou, L. Li, S. Chen, H.S. Park, Z.M. Wang, and G. Shen, Meters-Long Flexible CoNiO₂-Nanowires@Carbon-Fibers Based Wire-Supercapacitors for Wearable Electronics. *Advanced Materials Technologies* 2016. **1**(8), 1600142.
- [126] Zhang, Q., X. Wang, Z. Pan, J. Sun, J. Zhao, J. Zhang, C. Zhang, L. Tang, J. Luo, B. Song, Z. Zhang, W. Lu, Q. Li, Y. Zhang, and Y. Yao, Wrapping Aligned Carbon Nanotube Composite Sheets around Vanadium Nitride Nanowire Arrays for Asymmetric Coaxial Fiber-Shaped Supercapacitors with Ultrahigh Energy Density. *Nano Lett* 2017. **17**(4), 2719-2726.
- [127] Wang, Z., S. Qin, S. Seyedin, J. Zhang, J. Wang, A. Levitt, N. Li, C. Haines, R. Ovalle-Robles, W. Lei, Y. Gogotsi, R.H. Baughman, and J.M. Razal, High-Performance Biscrolled MXene/Carbon Nanotube Yarn Supercapacitors. *Small* 2018. e1802225.
- [128] Yang, Z., Y. Jia, Y. Niu, Z. Yong, K. Wu, C. Zhang, M. Zhu, Y. Zhang, and Q. Li, Wet-spun PVDF nanofiber separator for direct fabrication of coaxial fiber-shaped supercapacitors. *Chemical Engineering Journal* 2020. **400**,
- [129] Thavasi, V., G. Singh, and S. Ramakrishna, Electrospun nanofibers in energy and environmental applications. *Energy & Environmental Science* 2008. **1**(2), 205.
- [130] Bhattacharya, S., I. Roy, A. Tice, C. Chapman, R. Udangawa, V. Chakrapani, J.L. Plawsky, and R.J. Linhardt, High-Conductivity and High-Capacitance Electrospun Fibers for Supercapacitor Applications. *ACS Applied Materials & Interfaces* 2020. **12**(17), 19369-19376.
- [131] Yang, S., J. Ai, Z. Han, L. Zhang, D. Zhao, J. Wang, C. Yang, and B. Cao, Electrospun ZnFe₂O₄/carbon nanofibers as high-rate supercapacitor electrodes. *Journal of Power Sources* 2020. **469**, 228416.
- [132] Dai, Z., P.-G. Ren, Y.-L. Jin, H. Zhang, F. Ren, and Q. Zhang, Nitrogen-sulphur Co-doped graphenes modified electrospun lignin/polyacrylonitrile-based carbon nanofiber as high performance supercapacitor. *Journal of Power Sources* 2019. **437**, 226937.
- [133] Oner, E., Mechanical and Thermal Properties of Knitted Fabrics Produced from Various Fiber Types. *Fibers and Polymers* 2019. **20**(11), 2416-2425.
- [134] Chen, Y., B. Xu, J. Gong, J. Wen, T. Hua, C.W. Kan, and J. Deng, Design of High-performance Wearable Energy and Sensor Electronics from Fiber Materials. *ACS Appl Mater Interfaces* 2018.
- [135] Jost, K., D. Stenger, C.R. Perez, J.K. McDonough, K. Lian, Y. Gogotsi, and G. Dion, Knitted and screen printed carbon-fiber supercapacitors for applications in wearable electronics. *Energy & Environmental Science* 2013. **6**(9),
- [136] Sun, H., S. Xie, Y. Li, Y. Jiang, X. Sun, B. Wang, and H. Peng, Large-Area Supercapacitor Textiles with Novel Hierarchical Conducting Structures. *Adv Mater* 2016. **28**(38), 8431-8438.
- [137] Shen, C., Y. Xie, B. Zhu, M. Sanghadasa, Y. Tang, and L. Lin, Wearable woven supercapacitor

- fabrics with high energy density and load-bearing capability. *Sci Rep* 2017. **7**(1), 14324.
- [138] Rawal, A., Bending rigidity of thermally bonded nonwoven structures. *Fibers and Polymers* 2010. **11**(4), 654-660.
- [139] Kim, G.M., R. Lach, G.H. Michler, and Y.W. Chang, The mechanical deformation process of electrospun polymer nanocomposite fibers. *Macromolecular rapid communications* 2005. **26**(9), 728-733.
- [140] Pan, Z., J. Yang, L. Li, X. Gao, L. Kang, Y. Zhang, Q. Zhang, Z. Kou, T. Zhang, L. Wei, Y. Yao, and J. Wang, All-in-one stretchable coaxial-fiber strain sensor integrated with high-performing supercapacitor. *Energy Storage Materials* 2020. **25**, 124-130.
- [141] Sun, J., Y. Huang, C. Fu, Z. Wang, Y. Huang, M. Zhu, C. Zhi, and H. Hu, High-performance stretchable yarn supercapacitor based on PPy@CNTs@urethane elastic fiber core spun yarn. *Nano Energy* 2016. **27**, 230-237.
- [142] Mun, T.J., S.H. Kim, J.W. Park, J.H. Moon, Y. Jang, C. Huynh, R.H. Baughman, and S.J. Kim, Wearable Energy Generating and Storing Textile Based on Carbon Nanotube Yarns. *Advanced Functional Materials* 2020. **30**(23),
- [143] Sun, P., M. Qiu, M. Li, W. Mai, G. Cui, and Y. Tong, Stretchable Ni@NiCoP textile for wearable energy storage clothes. *Nano Energy* 2019. **55**, 506-515.
- [144] Park, H., J.W. Kim, S.Y. Hong, G. Lee, H. Lee, C. Song, K. Keum, Y.R. Jeong, S.W. Jin, D.S. Kim, and J.S. Ha, Dynamically Stretchable Supercapacitor for Powering an Integrated Biosensor in an All-in-One Textile System. *ACS Nano* 2019. **13**(9), 10469-10480.
- [145] Jun, J.H., H. Song, C. Kim, I.S. Choi, Y. Jeong, and J.H. Lee, Carbon-Nanosheet Based Large-Area Electrochemical Capacitor that is Flexible, Foldable, Twistable, and Stretchable. *Small* 2018. **14**(43), e1702145.
- [146] Liu, L., Q. Tian, W. Yao, M. Li, Y. Li, and W. Wu, All-printed ultraflexible and stretchable asymmetric in-plane solid-state supercapacitors (ASCs) for wearable electronics. *Journal of Power Sources* 2018. **397**, 59-67.
- [147] Gong, X., S. Li, and P.S. Lee, A fiber asymmetric supercapacitor based on FeOOH/PPy on carbon fibers as an anode electrode with high volumetric energy density for wearable applications. *Nanoscale* 2017. **9**(30), 10794-10801.
- [148] Uzun, S., S. Seyedin, A.L. Stoltzfus, A.S. Levitt, M. Alhabeb, M. Anayee, C.J. Strobel, J.M. Razal, G. Dion, and Y. Gogotsi, Knittable and Washable Multifunctional MXene - Coated Cellulose Yarns. *Advanced Functional Materials* 2019. **29**(45),
- [149] Van Lam, D., K. Jo, C.-H. Kim, S. Won, Y. Hwangbo, J.-H. Kim, H.-J. Lee, and S.-M. Lee, Calligraphic ink enabling washable conductive textile electrodes for supercapacitors. *Journal of Materials Chemistry A* 2016. **4**(11), 4082-4088.
- [150] Bellani, S., E. Petroni, A.E. Del Rio Castillo, N. Curreli, B. Martín - García, R. Oropesa - Nuñez, M. Prato, and F. Bonaccorso, Scalable Production of Graphene Inks via Wet - Jet Milling Exfoliation for Screen - Printed Micro - Supercapacitors. *Advanced Functional Materials* 2019. **29**(14),
- [151] Huang, Q., D. Wang, H. Hu, J. Shang, J. Chang, C. Xie, Y. Yang, X. Lepró, R.H. Baughman, and Z. Zheng, Additive Functionalization and Embroidery for Manufacturing Wearable and Washable Textile Supercapacitors. *Advanced Functional Materials* 2020.
- [152] Dong, L., C. Xu, Y. Li, Z. Pan, G. Liang, E. Zhou, F. Kang, and Q.H. Yang, Breathable and Wearable Energy Storage Based on Highly Flexible Paper Electrodes. *Adv Mater* 2016.

28(42), 9313-9319.

- [153] Chen, Y., K. Cai, C. Liu, H. Song, and X. Yang, High-Performance and Breathable Polypyrrole Coated Air-Laid Paper for Flexible All-Solid-State Supercapacitors. *Advanced Energy Materials* 2017. **7**(21),
- [154] Shin, D., C. Shen, M. Sanghadasa, and L. Lin, Breathable 3D Supercapacitors Based on Activated Carbon Fiber Veil. *Advanced Materials Technologies* 2018. **3**(11),
- [155] Yang, W. and X. Lu, Triboelectric Power Generation from Heterostructured Air - Laid Paper for Breathable and Wearable Self - Charging Power System. *Advanced Materials Technologies* 2019. **4**(12),
- [156] Wang, Y., Z. Pei, M. Zhu, Z. Liu, Y. Huang, Z. Ruan, Y. Huang, Y. Zhao, S. Du, and C. Zhi, A Wearable Supercapacitor Engaged with Gold Leaf Gilding Cloth Toward Enhanced Practicability. *ACS Appl Mater Interfaces* 2018. **10**(25), 21297-21305.
- [157] Cao, R., J. Wang, S. Zhao, W. Yang, Z. Yuan, Y. Yin, X. Du, N.-W. Li, X. Zhang, and X. Li, Self-powered nanofiber-based screen-print triboelectric sensors for respiratory monitoring. *Nano Research* 2018. **11**(7), 3771-3779.
- [158] Levitt, A., D. Hegh, P. Phillips, S. Uzun, M. Anayee, J.M. Razal, Y. Gogotsi, and G. Dion, 3D knitted energy storage textiles using MXene-coated yarns. *Materials Today* 2020. **34**, 17-29.
- [159] Levitt, A.S., M. Alhabeb, C.B. Hatter, A. Sarycheva, G. Dion, and Y. Gogotsi, Electrospun MXene/carbon nanofibers as supercapacitor electrodes. *Journal of Materials Chemistry A* 2019. **7**(1), 269-277.
- [160] Park, S., S. Ahn, J. Sun, D. Bhatia, D. Choi, K.S. Yang, J. Bae, and J.J. Park, Highly bendable and rotational textile structure with prestrained conductive sewing pattern for human joint monitoring. *Advanced Functional Materials* 2019. **29**(10), 1808369.
- [161] Lee, S.-S., K.-H. Choi, S.-H. Kim, and S.-Y. Lee, Wearable Supercapacitors Printed on Garments. *Advanced Functional Materials* 2018. **28**(11),
- [162] Chen, S., W. Ma, Y. Cheng, Z. Weng, B. Sun, L. Wang, W. Chen, F. Li, M. Zhu, and H.-M. Cheng, Scalable non-liquid-crystal spinning of locally aligned graphene fibers for high-performance wearable supercapacitors. *Nano Energy* 2015. **15**, 642-653.
- [163] Li, G.-X., P.-X. Hou, J. Luan, J.-C. Li, X. Li, H. Wang, C. Shi, C. Liu, and H.-M. Cheng, A MnO₂ nanosheet/single-wall carbon nanotube hybrid fiber for wearable solid-state supercapacitors. *Carbon* 2018. **140**, 634-643.
- [164] Wen, J., B. Xu, and J. Zhou, Towards 3D knitted-fabric derived supercapacitors with full structural and functional integrity of fiber and electroactive materials. *Journal of Power Sources* 2020. **473**,
- [165] Liu, L., Y. Feng, and W. Wu, Recent progress in printed flexible solid-state supercapacitors for portable and wearable energy storage. *Journal of Power Sources* 2019. **410-411**, 69-77.
- [166] Jin, H., L. Zhou, C.L. Mak, H. Huang, W.M. Tang, and H.L.W. Chan, High-performance fiber-shaped supercapacitors using carbon fiber thread (CFT)/polyaniline and functionalized CFT electrodes for wearable/stretchable electronics. *Nano Energy* 2015. **11**, 662-670.
- [167] Wang, Q., Y. Ma, X. Liang, D. Zhang, and M. Miao, Novel core/shell CoSe₂@PPy nanoflowers for high-performance fiber asymmetric supercapacitors. *Journal of Materials Chemistry A* 2018. **6**(22), 10361-10369.
- [168] Nagaraju, G., S.C. Sekhar, and J.S. Yu, Utilizing Waste Cable Wires for High-Performance Fiber-Based Hybrid Supercapacitors: An Effective Approach to Electronic-Waste

- Management. *Advanced Energy Materials* 2018. **8**(7),
- [169] Guo, J., Q. Zhang, J. Sun, C. Li, J. Zhao, Z. Zhou, B. He, X. Wang, P. Man, Q. Li, J. Zhang, L. Xie, M. Li, and Y. Yao, Direct growth of vanadium nitride nanosheets on carbon nanotube fibers as novel negative electrodes for high-energy-density wearable fiber-shaped asymmetric supercapacitors. *Journal of Power Sources* 2018. **382**, 122-127.
- [170] Li, P., Z. Jin, L. Peng, F. Zhao, D. Xiao, Y. Jin, and G. Yu, Stretchable All-Gel-State Fiber-Shaped Supercapacitors Enabled by Macromolecularly Interconnected 3D Graphene/Nanostructured Conductive Polymer Hydrogels. *Adv Mater* 2018. **30**(18), e1800124.
- [171] Li, B., J. Cheng, Z. Wang, Y. Li, W. Ni, and B. Wang, Highly-wrinkled reduced graphene oxide-conductive polymer fibers for flexible fiber-shaped and interdigital-designed supercapacitors. *Journal of Power Sources* 2018. **376**, 117-124.
- [172] Zhao, X., B. Zheng, T. Huang, and C. Gao, Graphene-based single fiber supercapacitor with a coaxial structure. *Nanoscale* 2015. **7**(21), 9399-404.
- [173] Wang, Q., X. Wang, J. Xu, X. Ouyang, X. Hou, D. Chen, R. Wang, and G. Shen, Flexible coaxial-type fiber supercapacitor based on NiCo₂O₄ nanosheets electrodes. *Nano Energy* 2014. **8**, 44-51.
- [174] Kang, Q., J. Zhao, X. Li, G. Zhu, X. Feng, Y. Ma, W. Huang, and J. Liu, A single wire as all-inclusive fully functional supercapacitor. *Nano Energy* 2017. **32**, 201-208.
- [175] Cao, X., Y. Liu, Y. Zhong, L. Cui, A. Zhang, J.M. Razal, W. Yang, and J. Liu, Flexible coaxial fiber-shaped asymmetric supercapacitors based on manganese, nickel co-substituted cobalt carbonate hydroxides. *Journal of Materials Chemistry A* 2020.
- [176] Luo, X., W. Weng, Y. Liang, Z. Hu, Y. Zhang, J. Yang, L. Yang, S. Yang, M. Zhu, and H.-M. Cheng, Multifunctional fabrics of carbon nanotube fibers. *Journal of Materials Chemistry A* 2019. **7**(15), 8790-8797.
- [177] Jost, K., D. Stenger, C.R. Perez, J.K. McDonough, K. Lian, Y. Gogotsi, and G. Dion, Knitted and screen printed carbon-fiber supercapacitors for applications in wearable electronics. *Energy & Environmental Science* 2013. **6**(9), 2698-2705.
- [178] Yu, X., X. Su, K. Yan, H. Hu, M. Peng, X. Cai, and D. Zou, Stretchable, Conductive, and Stable PEDOT-Modified Textiles through a Novel In Situ Polymerization Process for Stretchable Supercapacitors. *Advanced Materials Technologies* 2016. **1**(2), 1600009.
- [179] Han, Y., Y. Lu, S. Shen, Y. Zhong, S. Liu, X. Xia, Y. Tong, and X. Lu, Enhancing the Capacitive Storage Performance of Carbon Fiber Textile by Surface and Structural Modulation for Advanced Flexible Asymmetric Supercapacitors. *Advanced Functional Materials* 2019. **29**(7),
- [180] Wang, L., C. Zhang, X. Jiao, and Z. Yuan, Polypyrrole-based hybrid nanostructures grown on textile for wearable supercapacitors. *Nano Research* 2019. **12**(5), 1129-1137.
- [181] Qiang, S., T. Carey, A. Arbab, W. Song, C. Wang, and F. Torrisi, Wearable solid-state capacitors based on two-dimensional material all-textile heterostructures. *Nanoscale* 2019. **11**(20), 9912-9919.
- [182] Guo, R., J. Li, Y. Jia, F. Xin, J. Sun, L. Dang, Z. Liu, and Z. Lei, Nitrogen-doped carbon sheets coated on CoNiO₂@textile carbon as bifunctional electrodes for asymmetric supercapacitors. *Journal of Materials Chemistry A* 2019. **7**(8), 4165-4174.
- [183] Li, D.-J., S. Lei, Y.-Y. Wang, S. Chen, Y. Kang, Z.-G. Gu, and J. Zhang, Helical carbon tubes derived from epitaxial Cu-MOF coating on textile for enhanced supercapacitor performance. *Dalton Transactions* 2018. **47**(16), 5558-5563.

- [184] Jin, L.-N., F. Shao, C. Jin, J.-N. Zhang, P. Liu, M.-X. Guo, and S.-W. Bian, High-performance textile supercapacitor electrode materials enhanced with three-dimensional carbon nanotubes/graphene conductive network and in situ polymerized polyaniline. *Electrochimica Acta* 2017. **249**, 387-394.
- [185] Singh, S.B., T.I. Singh, N.H. Kim, and J.H. Lee, A core-shell MnO₂@Au nanofiber network as a high-performance flexible transparent supercapacitor electrode. *Journal of Materials Chemistry A* 2019. **7**(17), 10672-10683.
- [186] Wen, J., B. Xu, J. Zhou, J. Xu, and Y. Chen, 3D Patternable Supercapacitors from Hierarchically Architected Porous Fiber Composites for Wearable and Waterproof Energy Storage. *Small* 2019. **15**(25), e1901313.
- [187] Li, X., X. Chen, Y. Zhao, Y. Deng, J. Zhu, S. Jiang, and R. Wang, Flexible all-solid-state supercapacitors based on an integrated electrode of hollow N-doped carbon nanofibers embedded with graphene nanosheets. *Electrochimica Acta* 2020. **332**,
- [188] Pan, Q., E. Shim, B. Pourdeyhimi, and W. Gao, Highly Conductive Polypropylene-Graphene Nonwoven Composite via Interface Engineering. *Langmuir* 2017. **33**(30), 7452-7458.
- [189] Lin, Y., Y. Gao, and Z. Fan, Printable Fabrication of Nanocoral-Structured Electrodes for High-Performance Flexible and Planar Supercapacitor with Artistic Design. *Adv Mater* 2017. **29**(43),
- [190] Lu, Q., L. Liu, S. Yang, J. Liu, Q. Tian, W. Yao, Q. Xue, M. Li, and W. Wu, Facile synthesis of amorphous FeOOH/MnO₂ composites as screen-printed electrode materials for all-printed solid-state flexible supercapacitors. *Journal of Power Sources* 2017. **361**, 31-38.
- [191] Zhang, H., Y. Qiao, and Z. Lu, Fully Printed Ultraflexible Supercapacitor Supported by a Single-Textile Substrate. *ACS Appl Mater Interfaces* 2016. **8**(47), 32317-32323.
- [192] Liu, L., Y. Feng, J. Liang, S. Li, B. Tian, W. Yao, and W. Wu, Structure-designed fabrication of all-printed flexible in-plane solid-state supercapacitors for wearable electronics. *Journal of Power Sources* 2019. **425**, 195-203.
- [193] Huang, Q., D. Wang, and Z. Zheng, Textile-Based Electrochemical Energy Storage Devices. *Advanced Energy Materials* 2016. **6**(22), 1600783.
- [194] Sun, H., L. Mei, J. Liang, Z. Zhao, C. Lee, H. Fei, M. Ding, J. Lau, M. Li, and C. Wang, Three-dimensional holey-graphene/niobia composite architectures for ultrahigh-rate energy storage. *Science* 2017. **356**(6338), 599-604.
- [195] Simon, P., Y. Gogotsi, and B. Dunn, Materials science. Where do batteries end and supercapacitors begin? *Science* 2014. **343**(6176), 1210-1.
- [196] Feng, D.-Y., Z. Sun, Z.-H. Huang, X. Cai, Y. Song, and X.-X. Liu, Highly loaded manganese oxide with high rate capability for capacitive applications. *Journal of Power Sources* 2018. **396**, 238-245.
- [197] Kim, J.H., C. Choi, J.M. Lee, M.J. de Andrade, R.H. Baughman, and S.J. Kim, Ag/MnO₂ composite sheath-core structured yarn supercapacitors. *Scientific reports* 2018. **8**(1), 1-8.
- [198] Ortaboy, S., J.P. Alper, F. Rossi, G. Bertoni, G. Salvati, C. Carraro, and R. Maboudian, MnO_x-decorated carbonized porous silicon nanowire electrodes for high performance supercapacitors. *Energy & Environmental Science* 2017. **10**(6), 1505-1516.
- [199] Cheng, H.-M. and F. Li, Charge delivery goes the distance. *Science* 2017. **356**(6338), 582-583.
- [200] Gambou-Bosca, A. and D. Bélanger, Chemical mapping and electrochemical performance of manganese dioxide/activated carbon based composite electrode for asymmetric

- electrochemical capacitor. *Journal of The Electrochemical Society* 2015. **162**(5), A5115.
- [201] Shang, J., Q. Huang, L. Wang, Y. Yang, P. Li, and Z. Zheng, Soft Hybrid Scaffold (SHS) Strategy for Realization of Ultrahigh Energy Density of Wearable Aqueous Supercapacitors. *Adv Mater* 2020. **32**(4), e1907088.
- [202] Yun, T.G., B. Hwang, D. Kim, S. Hyun, and S.M. Han, Polypyrrole-MnO(2)-Coated Textile-Based Flexible-Stretchable Supercapacitor with High Electrochemical and Mechanical Reliability. *ACS Appl Mater Interfaces* 2015. **7**(17), 9228-34.
- [203] Anasori, B., M.R. Lukatskaya, and Y. Gogotsi, 2D metal carbides and nitrides (MXenes) for energy storage. *Nature Reviews Materials* 2017. **2**(2),
- [204] Sun, N., Q. Zhu, B. Anasori, P. Zhang, H. Liu, Y. Gogotsi, and B. Xu, MXene - Bonded Flexible Hard Carbon Film as Anode for Stable Na/K - Ion Storage. *Advanced Functional Materials* 2019. **29**(51),
- [205] Zhang, C.J., M.P. Kremer, A. Seral-Ascaso, S.-H. Park, N. McEvoy, B. Anasori, Y. Gogotsi, and V. Nicolosi, Stamping of Flexible, Coplanar Micro-Supercapacitors Using MXene Inks. *Advanced Functional Materials* 2018. **28**(9),
- [206] Lv, J., I. Jeerapan, F. Tehrani, L. Yin, C.A. Silva-Lopez, J.-H. Jang, D. Joshua, R. Shah, Y. Liang, L. Xie, F. Soto, C. Chen, E. Karshalev, C. Kong, Z. Yang, and J. Wang, Sweat-based wearable energy harvesting-storage hybrid textile devices. *Energy & Environmental Science* 2018. **11**(12), 3431-3442.
- [207] Cheng, Q., C. Meng, Y. Qian, J. He, and X. Dong, Energy capacity enhancement of all-organic fabric supercapacitors by organic dyes: Old method for new application. *Progress in Organic Coatings* 2020. **138**,
- [208] Fard, H.N., G.B. Pour, M.N. Sarvi, and P. Esmaili, PVA-based supercapacitors. *Ionics* 2019. **25**(7), 2951-2963.
- [209] Huang, Y., M. Zhong, F. Shi, X. Liu, Z. Tang, Y. Wang, Y. Huang, H. Hou, X. Xie, and C. Zhi, An Intrinsically Stretchable and Compressible Supercapacitor Containing a Polyacrylamide Hydrogel Electrolyte. *Angew Chem Int Ed Engl* 2017. **56**(31), 9141-9145.
- [210] Tang, Y., X. Li, H. Lv, D. Xie, W. Wang, C. Zhi, and H. Li, Stabilized Co³⁺/Co⁴⁺ Redox Pair in In Situ Produced CoSe₂-x - Derived Cobalt Oxides for Alkaline Zn Batteries with 10 000 - Cycle Lifespan and 1.9 - V Voltage Plateau. *Advanced Energy Materials* 2020. 2000892.
- [211] Yang, Y., Q. Huang, L. Niu, D. Wang, C. Yan, Y. She, and Z. Zheng, Waterproof, ultrahigh areal - capacitance, wearable supercapacitor fabrics. *Advanced Materials* 2017. **29**(19), 1606679.
- [212] Xu, P., T. Gu, Z. Cao, B. Wei, J. Yu, F. Li, J.H. Byun, W. Lu, Q. Li, and T.W. Chou, Carbon Nanotube Fiber Based Stretchable Wire - Shaped Supercapacitors. *Advanced Energy Materials* 2014. **4**(3),
- [213] Niu, Q., K. Gao, and Z. Shao, Cellulose nanofiber/single-walled carbon nanotube hybrid non-woven macrofiber mats as novel wearable supercapacitors with excellent stability, tailorability and reliability. *Nanoscale* 2014. **6**(8), 4083-8.
- [214] Qin, S., S. Seyedin, J. Zhang, Z. Wang, F. Yang, Y. Liu, J. Chen, and J.M. Razal, Elastic Fiber Supercapacitors for Wearable Energy Storage. *Macromol Rapid Commun* 2018. **39**(13), e1800103.
- [215] Jang, Y., S.M. Kim, G.M. Spinks, and S.J. Kim, Carbon Nanotube Yarn for Fiber - Shaped Electrical Sensors, Actuators, and Energy Storage for Smart Systems. *Advanced Materials* 2020. **32**(5), 1902670.